ANEXO 8

Cloud processes of the main precipitation systems in Brazil: Overview and first results from the CHUVA project

Marc Schneebeli[1], Johjy Sakuragi[1], Carlos Morales[2], Carlos Angelis[1], Luiz Machado[1], Luca Baldini[3]
[1]National Institute for Space Research (INPE), Center for Weather Forecasting and Climate Studies (CPTEC), Cachoeira Paulista/SP, Brazil
[2]Sao Paulo
[3]Italy

In April 2011, the first field campaign of the CHUVA project took place in Fortaleza, on the norh-eastern coast of Brazil. The set-up of remote sensors consisted of an X-band polarimetric weather radar, a Ka-band Micro Rain Radar, a Raman lidar, and a passive microwave temperature and humidity profiler and was complemented by a wealth of ground-based (disdrometers, rain gauges, anemometric tower) and air-borne (triangle of radiosonde launches every six hours, research aircraft with particle detection) in-situ sensors. With this unprecedented sensor assembly deployed in the tropics, a detailed assessment of processes governing the formation of clouds and precipitation becomes feasible. The focus on the first campaign in Fortaleza is put on the detection of warm clouds, i.e., clouds that do not exceed the melting layer and therefore form precipitation without the influence of the ice phase. Rain events originating from warm clouds can be very hazardous, but detection with traditional satellite-based precipitation estimation schemes is difficult due to the lack of the ice phase of these clouds and therefore remains an unresolved problem. It is expected that the results from the Fortaleza campaign will improve the understanding of warm rain events and eventually lead to better rain estimates over land. Following the campaign in Fortaleza, the whole sensor assembly will be moved to Belem, a city in the north of Brazil, at the border of the Amazon and just slightly below the Equator. The focus of the Belem campaign, taking place in June and July 2011, is put on tropical squall-lines and their associated processes that form intense tropical precipitation.
We will present an overview of the CHUVA project and first results obtained from the campaigns in Fortaleza and Belem. First data analysis includes the assessment of the performance of different radar attenuation correction schemes with respect to the variety of rain types. In addition, the behavior of the vertical profiles of polarimetric observables during different meteorological situations is studied.

ANEXO 9

Available online at www.sciencedirect.com
ScienceDirect
Advances in Space Research xxx (2011) xxx–xxx
ADVANCES IN SPACE RESEARCH (a COSPAR publication)
www.elsevier.com/locate/asr

Radiometric estimation of water vapor content over Brazil

P.K. Karmakar [a], M. Maiti [b,*], S. Sett [a], C.F. Angelis [c], L.A.T. Machado [c]

[a] Centre for Research and Training in Microwave and Millimeter wave, Institute of Radiophysics and Electronics, University of Calcutta, 92. A.P.C Road, Kolkata 700 009, India
[b] MCKV Institute of Engineering, 243, G.T Road (North), Liluah, Howrah 711204, India
[c] Instituto Nacional de Pesquisas Espaciais-INPE, Centro de Previsão de Tempo e studos, Climáticos-CPTEC-Road, Dutra, km 40, Cachoeira Paulista, SP 12630000, Brazil

Received 9 March 2011; received in revised form 22 June 2011; accepted 30 June 2011

Abstract

A multi-channel microwave radiometre (make: Radiometrics Corporation) is installed at Instituto Nacional de Pesquisas Espaciais–INPE, Brazil (22°S). The radiometric output of two channels of the radiometer in the form of brightness temperature at 23.834 GHz and 30 GHz, initially, were used to find out the ambient water vapor content and the non-precipitable cloud liquid water content. The necessary algorithm was developed for the purpose. The best results were obtained using the hinge frequency 23.834 GHz and 30 GHz pair having an r.m.s. error of only 2.64. The same methodology was then adopted exploiting 23.034 GHz and 30 GHz pair. In that case the r.m.s. error was 3.42. These results were then compared with those obtained over Kolkata (22°N), India, by using 22.234 GHz and 31.4 GHz radiometric data. This work conclusively suggests the use of a frequency should not be at the water vapor resonance line. Instead, while measuring the vapor content for separation of vapor and cloud liquid, one of them should be a few GHz left or right from the resonance line i.e., at 23.834 GHz and the other one should be around 30 GHz.

Keywords: Dual frequency; Radiosonde; Radiometer; Water vapor; Liquid water

1. Introduction

Out of all meteorological parameters, water vapor and non-precipitable liquid water along with ambient temperature are found to be the most important ones to control thermodynamic balance, photochemistry of the atmosphere, sun-weather relationship and the biosphere as well. Measurements of the vertical and horizontal distribution of water vapor, as well as its temporal variation are essential for probing into the mysteries of several atmospheric effects. A sizeable literature has focused on the complex relationship between water vapor variability and deep convection in the tropics (Sherwood et al., 2009). Unlike higher latitudes, rotational dynamical constraints are weak and precipitation-induced heating perturbations are rapidly communicated over great distances. Water vapor, on the other hand, is highly variable in space and time; its spatial distribution depending on much slower advection processes above the boundary layer and on deep convection itself. Furthermore, deep convection, through vertical transport of water vapor and evaporation of cloud droplets and hydrometeors, serves as the free tropospheric water vapor source. And deep convection is itself sensitive to the free tropospheric humidity distribution through local moistening of the environment which favors further deep convection; a positive feedback (David et al., 2011). In this context, the ground based microwave radiometric sensing appears to be one of the suitable solutions for continuous monitoring of ambient atmospheric water vapor. Radiometric data have been extensively used by several investigators (Westwater, 1972; Gordy, 1976; Westwater and

* Corresponding author. Tel.: +91 9434972024.
E-mail addresses: karmakar_p_k@yahoo.com, pkarmakar745@gmail.com (P.K. Karmakar), manab1972@yahoo.com, manabendramaiti@gmail.com (M. Maiti), carlos.angelis@cptec.inpe.br (C.F. Angelis).

0273-1177/$36.00 © 2011 COSPAR. Published by Elsevier Ltd. All rights reserved.
doi:10.1016/j.asr.2011.06.032

Guiraud, 1980; Pandey et al., 1984; Janssen, 1985; Cimini et al., 2007) to determine water vapor budget. The prime objective of this work is to measure atmospheric water vapor and cloud liquid water content by deploying the ground based radiometric technique and subsequently to compare the results with those derived by using radiosonde data.

The first absorption maxima although weak, in the microwave band occur at 22.234 GHz. So, one can have the choice of exploiting 22.234 GHz on the basis of assumption that the signal to noise ratio is largest at this frequency, provided the vertical profiles of pressure and temperature are constant (Resch, 1983). But this does not happen in practice. Pressure and temperature are highly variable parameters of the atmosphere. In this connection, Westwater (1978), showed that the frequency independent of pressure lie both way around the resonance line i.e., 22.234 GHz. This single frequency measurement of water vapor was done by Karmakar et al. (1999) at Kolkata (22°N) and at Instituto Nacional de Pesquisas Espaciais (INPE), Cachoeira Paulista (CP), (22°S) Brazil, Karmakar et al. (2010). But incidentally, 22.235 GHz is affected by pressure broadening although the resonance peak occurs there and these measurements were not devoid of any influence by the presence of overhead cloud liquid. It has been shown (Simpson et al., 2002) that a zenith-pointing ground-based microwave radiometer measuring sky brightness temperature in the region of 22 GHz is three times more sensitive to the amount of water vapor than the amount of liquid water. However, in the region of 30 GHz, the sky brightness temperature is two times more sensitive to liquid water than that of water vapor, taking into consideration that the sensitivity to ice is negligible at both the frequencies.

Keeping these in view, the present authors were prompted to use dual frequency radiometric measurement of water vapor at Instituto Nacional de Pesquisas Espaciais (INPE), Cachoeira Paulista (CP), Brazil (22°S) exploiting 23.834 GHz and 30 GHz pair. The measurement of water vapor at Kolkata was also done by exploiting 22.235 GHz and 30 GHz pair (Karmakar et al., 2001). But in the present context, the authors are using two more frequency pairs to get the improved desired accuracy of retrieving vapor at the place of choice. Here, the present authors have chosen 23.834 GHz (hinge frequency) because of its independent nature of pressure broadening to get rid of unwanted signal in the vicinity of 23.834 GHz. Moreover, an attempt has also been made to use 23.034, a few GHz away from the peak line frequency (refer to Fig. 1) and 30 GHz pair.

In the tropical region, the data on cloud liquid water are quite inadequate, particularly in view of strong seasonal dependence associated with the monsoon (Maitra and Chakraborty, 2009). In the present paper, liquid water (LWC) has also been obtained from dual frequency radiometric measurements at a tropical location to indicate its variational pattern. Besides this, it may be mentioned that although the latitudinal occupancy [Kolkata 22°N, India; CP, 22°S, Brazil], of both the places are the same, the measurement of vapor draws a special attention because of entirely different environmental conditions, especially due to presence of Amazon Basin.

The necessary data for the purpose were available from the multi-channel microwave radiometer installed at Instituto Nacional de Pesquisas Espaciais (INPE), Cachoeira Paulista, Brazil (22°S).

2. Instrumentation and data processing

The radiometer has been designed for ease of use, accuracy, reliability, portability, etc. As in this case the radiometric technique is a passive technology, it does not emit radiation detectable by any normal means. The MP-3000A series radiometer consists of 35 channels. This radiometer incorporates two radio frequency (RF) subsystems in the same cabinet. These RF subsystems share the same antenna and antenna profiling system. The water vapor band utilizes sky brightness temperature observations at selected frequencies between 22 and 30 GHz. The antenna system has a clear view of the sky from horizon to horizon, at least in one vertical plane. However, in our case, the antenna is pointed towards the zenith. The radiometer is controlled by radiometrics proprietary software. Calibration is done using liquid nitrogen and displayed in graphical format. There are three options in the main menu of the software: level '0' files (raw sensor data in volts), level '1' files (brightness temperatures) and level '2' files (profile retrievals). Here, in our study we have used only the level '1' file. The radiometer outputs in the level '1' file were taken in the form of sky brightness temperature (T_B). Care has been taken for proper calibration of the radiometer between the cold source (built into the radiometer) and sky brightness temperature.

The total attenuation was calculated from the measured brightness temperatures at the desired frequencies by using the relation given by Allnutt (1976)

$$A(\mathrm{dB}) = 10log_{10}\frac{T_m - T_{cos}}{T_m - T_B} \tag{1}$$

Here T_m is the mean atmospheric temperature in K; T_{cos} is the cosmic background whose value is taken as 2.7 K and T_B is the brightness temperature in K. To evaluate the mean atmosphere temperature T_m, we take help of radiative transfer equation of Chandrasekhar for non-scattering and non-refractive atmosphere where the mean atmospheric temperature is given by

$$T_m = \frac{T_B}{\int \alpha_v exp[\tau_v(0,z)]dz} \tag{2}$$

where T_B is the equivalent brightness temperature and is given by Ulaby et al. (1986)

$$T_B = \int_0^\infty \alpha_v(z)T(z)\left[exp\left\{-\int_0^z \alpha_v(z)dz\right\}\right]dz \tag{3}$$

and $\tau_v(0,z) = \int_0^z \alpha_v(z)dz$, known as zenith opacity.

Please cite this article in press as: Karmakar, P.K., et al. Radiometric estimation of water vapor content over Brazil. J. Adv. Space Res. (2011), doi:10.1016/j.asr.2011.06.032

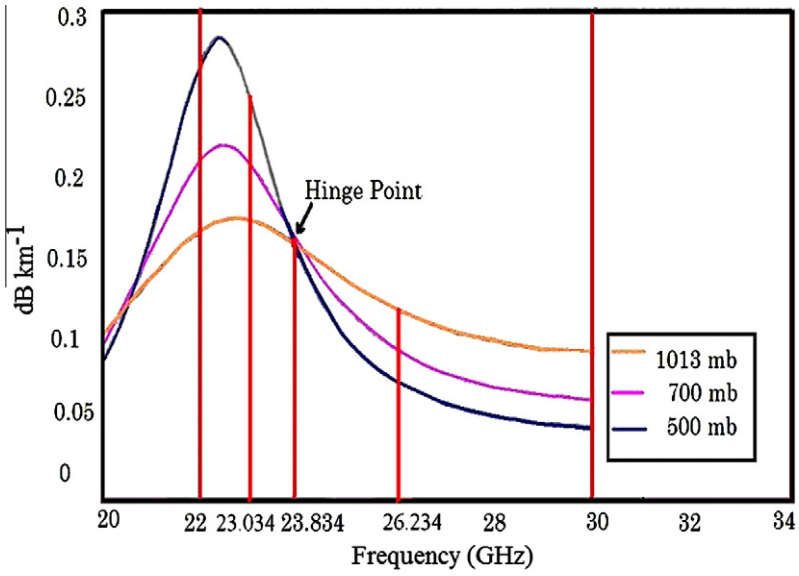

Fig. 1. Representative plot of showing the occurrence of pressure independent frequency 23.834 GHz.

Here, the mean atmospheric temperature is a frequency dependent parameter. It can be found with the help of known vertical profile of atmospheric temperature and the corresponding vertical profile of attenuation (dB km^{-1}) at the desired frequencies. In fact the integration in this Eq. (24) has been carried out in the height interval 0–10 km because beyond 10 km the abundance of water vapor is negligibly small as shown by Evans and Hagfors (1968).

2.1. Radiometer specification: model MP-3000A

Brightness temperature range (K) = 0–400
Calibrated brightness temperature accuracy (K) = 0.5
Long-term stability (K $year^{-1}$) < 1.0
Integration time (s) (user selectable in 10 ms increments) = 0.01–2.5
Resolution (K) (depends on integration time) = 0.1–1
Antenna characteristics 22 GHz 30 GHz
Half power beam width (°) = 6.3 (22 GHz), 4.9 (30 GHz)
Gain (dBi) = 30 (22 GHz), 32 (30 GHz)
Side lobes (dB) < −23 (22 GHz), <−24 (30 GHz)
Pre-detection channel bandwidth (MHz) (effective RF bandwidth) = 300

3. Theoretical background

Atmospheric attenuation in the microwave region is mainly due to water vapor, liquid water, and gaseous particles (mainly oxygen). Amongst these, water vapor plays a major role in attenuating the microwave signal during its propagation through the ambient atmosphere. Microwave signal gets also attenuated in the presence of cloud containing liquid water. Gaseous oxygen, though not as intense as water, contributes to the attenuation. Now, the total attenuation in dB is written mathematically as

$$A_T = A_V(f) + A_L(f) + A_0(f) \tag{4}$$

Here, A_T is the total attenuation, A_V is the attenuation due to water vapor, A_L is the attenuation due to non-precipitable cloud liquid water and A_0 is the attenuation due to oxygen. Now using Eq. (1), the total attenuation for the higher frequency (f_2) can be formulated as

$$A_T = A_V(f_2) + A_L(f_2) + A_0(f_2) \tag{5}$$

Similarly, the total attenuation involving frequency f_1, (the lesser one) can be written as

$$A_T = A_V(f_1) + A_L(f_1) + A_0(f_1) \tag{6}$$

Attenuation due to cloud liquid at the two frequencies are related as (Karmakar et al., 2001)

$$A_L(f_2) = K_1 A_L(f_1) \tag{7}$$

where $K_1 = (f_2/f_1)^2$.

Multiplying relation (6) by K_1 we get,

$$K_1 A_T(f_1) = K_1 A_L(f_1) + K_1 A_0(f_1) + K_1 A_V(f_1) \tag{8}$$

From (5) and (8) and rearranging we get

$$[K_1 A_T(f_1) - A_T(f_2)] - [K_1 A_0(f_1) - A_0(f_2)] = K_1 A_V(f_1) - A_V(f_2) \tag{9}$$

Now we choose the left hand side of Eq. (9), to be written as

$$Z_V = [K_1 A_T(f_1) - K_1(f_2)] - [K_1 A_0(f_1) - A_0(f_2)] \tag{10}$$

Here we see that the term Z_V contains only the vapor part and dry part and can be termed as attenuation part free from liquid attenuation.

Please cite this article in press as: Karmakar, P.K., et al. Radiometric estimation of water vapor content over Brazil. J. Adv. Space Res. (2011), doi:10.1016/j.asr.2011.06.032

A statistical regression analysis between the calculated values of water vapor attenuation $A_V(f_1)$ and $A_V(f_2)$ by using radiosonde data reveals that they are related as

$$A_V(f_2) = K_2 A_V(f_1) \tag{11}$$

where K_2 is the regression constant

Again, involving Eq. (7), and progressing similar to the case of water vapor we get

$$Z_L = [A_T(f_2) - \{K_2 A_T(f_1)\}] - [A_0(f_2) - \{K_2 A_0(f_1)\}] \tag{12}$$

4. Radiosonde data analysis of vapor estimation

We define the mass of water vapor content in a cylindrical column of one square meter cross-sectional base area as Integrated Precipitable Water Vapor (IPVP), expressed in kg m^{-2}. Similarly, liquid water is the depth of water that could be collected from a column of cloud liquid water droplets which can also be expressed in kg m^{-2}.

This measurement cannot be done analytically. So it is accomplished by constructing a database of water vapor content, liquid water content and the brightness temperature values. The amount of water vapor contained in the atmosphere is a function of several meteorological parameters, but it specially depends on the atmospheric temperature. The primary parameter of interest in finding the water vapor density is the partial water vapor pressure (mb) which is given by the relation (Moran and Rosen, 1981)

$$e = 6.10 exp\{25.228(1 - (273/T_D)) - (5.31 log(T_D/273))\} \tag{13}$$

where T_D is the dew point in °K.

But, during saturation this water vapor pressure can be formulated as

$$e_s = 6.112 \frac{exp(17.502 \times t)}{t + 240.97} mb \tag{14}$$

where t is the atmospheric temperature in °C.

Now, one can take the liberty to consider that water vapor approximately behaves as an ideal gas, where each mole of gas obeys an equation of state that can be written as

$$\rho_v = e/R_w T \tag{15}$$

where ρ_v is the water vapor density (kg m^{-2})and e is the partial pressure of water vapor (mb). R_w is the gas constant for water vapor i.e., $R_w = R/m_w$, where R is the universal gas constant and m_w is the mass of one mole of vapor, and T the absolute temperature (°K). Here $R = 8.135$ J/mole °K and $m_w = 18$ gm. Substituting all these above values in Eq. (15), we find the water vapor density (gm m^{-3}).

$$\rho_v = \frac{1800e}{8.3145T} \tag{16}$$

Usually ρ_v is multiplied by 10^3 and expressed in kg m^{-3}.

Each radiosonde ascent records profiles of atmospheric pressure, altitude, temperature and dew point temperature data. In the standard data format used, all four quantities are recorded generally, at 15 specified values of atmospheric pressure. Intermediate values may be recorded whenever there are significant changes of pressure or temperature at corresponding altitudes. It can be determined by interpolation, assuming an exponential profile between the relevant pressure values. Vertical profiles that match the slab heights required by the Liebe's model are then obtained by further interpolation. It is to be noted that the atmosphere may divided into 0.2 km thick slab and above 5 km it has been assumed as 1 km thick. The pressure, temperature and dew point temperature at each height are used to derive relative humidity, air density and vapor pressure for each slab. From these we may obtain the water vapor density profile, and hence vapor content by integration with respect to height.

In the present context, we are interested in finding the integrated water vapor content, defined earlier, that can be written as

$$V(\text{kg m}^{-2}) = \int_0^\infty \rho_v(h) dh \tag{17}$$

Water vapor absorption coefficients, (α_V dB km^{-1}) at the corresponding heights are obtained using Leibe's MPM model (Liebe, 1985). The data inputs are temperature, pressure and R_H which is given by $R_H = \frac{e}{e_s} \times 100$.

5. Radiosonde data analysis of cloud attenuation

We are usually accustomed with different types of cloud discussed by several authors from time to time along with their generation and formation mechanism. Amongst those types of clouds, we were concerned with clouds when the radiometric temperatures were little higher in presence of cloud. These types of cloud sometimes extend well above the cirrus type and penetrate a few thousand feet into the stratosphere. The water content of cloud normally increases upward to a maximum in the vicinity of melting level. These types contain exceedingly high vertical velocities and in that case the presence of hail above the tropopause also is possible.

But, it is to be pointed out that such steady state conditions with respect to water distribution in the cloud do not exist when updrafts equal or exceed the fall velocity of particle as rain. Such updrafts exist only locally for periods about 5–15 min in convective activity (David et al., 2011) and hence can lead to high local concentration of water. However, the calculation of the columnar liquid water content of clouds from radiosonde measurements is based on the model proposed by (Salonen, 1991).

The cloud detection is performed using the "critical humidity" function defined as follows:

$$U_C = 1 - \sigma\alpha(1 - \sigma)[1 + \beta(\sigma - 0.5)] \tag{18}$$

Here $\sigma = p/p_0$ = ratio between the atmospheric pressure at the considered level and the pressure at the ground where $\alpha = 1.0$ and, $\beta = \sqrt{3}$, (an empirical constant) as proposed

Please cite this article in press as: Karmakar, P.K., et al. Radiometric estimation of water vapor content over Brazil. J. Adv. Space Res. (2011), doi:10.1016/j.asr.2011.06.032

by Salonen (1991). In Silverman and Sprague's model used earlier by Karmakar et al. (2001) at Kolkata, it was presumed that the distribution of liquid water within the cloud thickness ranging from 660 m to 3.4 km was not uniform (no actual profile was mentioned) without having any prior knowledge of cloud thickness over Kolkata. But in Salonen model, the cloud thickness can easily be evaluated by using Fig. 2 where in cloud base and top were found to be 1.5 km and 3.0 km and distribution were taken as uniform. This helps us to provide the proper integration limit while retrieving vapor separating liquid content.

Besides these in Salonen model no hail or ice cloud were taken into consideration which favors the choice of this model over Brazil. Salonen proposed this model for cloud water density in terms of temperature and height from cloud base that can be used to obtain the liquid water density profile within cloud.

The existence of cloud at the certain level were taken into consideration when the relative humidity at a particular height is greater than the U_C, as mentioned in Eq. (18). Again it is presumed that within the cloud layer the water density ρ_C, of any slice of the upper air sounding is a function of the air temperature, t (°C), and of the layer height, h (m). The existence of cloud at the certain level was taken into consideration when the relative humidity at a particular height is greater than the U_C. The plot of the vertical profile of $U_C(h)$ and R_H for a particular day, dated 10 April 2009, over Brazil, for the sake of clarity, is presented in Fig. 2. The cloud base height and the cloud top height are found by interpolation method as shown in the same figure. Here h_1 is the base height of the cloud where the RH curve crosses the $U_C(h)$ curve for the first time. The cloud top h_2 is the point on the curve where the curve $U_C(h)$ again crosses the R_H curve. Again it is presumed that within the cloud layer the water density ρ_C, of any slice

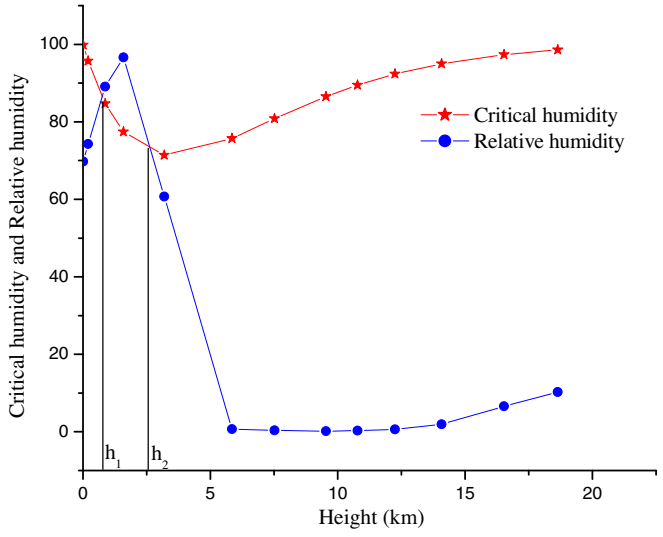

Fig. 2. Curve illustrating the method to find the heights between which cloud exits.

of the upper air sounding is a function of the air temperature, t (°C), and of the layer height, h (m). It is given by

$$\rho_C(t,h) = \rho_0 exp(Ct)\left(\frac{h-h_b}{h_r}\right)\rho_w \tag{19}$$

where, $\rho_0 = 0.17$ (gm m^{-3}); $C = 0.04$ (°C^{-1}) and is a temperature dependence factor; $h_r = 1500$ (m) and $h_b =$ cloud base height (m).

And $p_w(t)$ is the liquid water fraction, approximated by

$$p_w(t) = 1 \text{ if } 0\,^\circ\text{C} < t$$
$$p_w(t) = 1 + t/20 \text{ if } -20\,^\circ\text{C} < t < 0\,^\circ\text{C}$$
$$p_w(t) = 0 \text{ if } t < -20\,^\circ\text{C}$$

Here it is to be mentioned that Eq. (19) was the key equation derived by Salonen (1991). This model was also used by Maitra and Chakraborty (2009) for Kolkata by using the radiosonde data only.

The calculation of both cloud base and top heights may be worked out from ground by linear interpolation. The columnar liquid water content, L, can be found by adding the contributions from all the layers within the clouds that contain water.

The total liquid water content is given by

$$L(\text{kg m}^{-2}) = \int_{h_1}^{h_2} \rho_C(h)dh \tag{20}$$

Here, it is to be noted over Brazil (22°S), the h_2 values were different for different days. But the maximum value of h_2 was found as 3 kms. So it is conclusively decided that over Brazil, the cloud never was extended up to stratosphere and question does not arise of formation of hail above the tropopause.

For clouds consisting entirely of small droplets, generally less than 0.01 cm, the Rayleigh approximation is valid for frequencies below 200 GHz and it is possible to express the attenuation in terms of the total water content per unit volume. Thus the specific attenuation within a cloud can be written as

$$\alpha_C = K_L \rho_C \tag{21}$$

(where, $\alpha_C =$ specific attenuation (dB km^{-1}) within the cloud; $K_L =$ specific attenuation coefficient (dB km^{-1}/gm m^{-3}) and $\rho_C =$ liquid water density in the cloud (gm m^{-3}).

A mathematical model based on Rayleigh absorption for non-precipitating clouds, we assume the liquid absorption depends only on the total liquid amount and does not depend on the drop size distribution. The Rayleigh approximation is valid when the scattering parameter much less than one which uses a double-Debye model for the dielectric permittivity $\mathcal{E}(f)$ of water. This idea can be used to calculate the value of K_L for frequencies up to 1000 GHz where

$$K_L = \frac{0.819f}{\varepsilon''(1+\eta)^2} \tag{22}$$

and f is the frequency (GHz), and $\eta = \frac{2+\varepsilon'}{\varepsilon''}$.

Please cite this article in press as: Karmakar, P.K., et al. Radiometric estimation of water vapor content over Brazil. J. Adv. Space Res. (2011), doi:10.1016/j.asr.2011.06.032

The complex dielectric permittivity of water is given by

$$\varepsilon''(f) = \frac{f(\varepsilon_0 - \varepsilon_1)}{fp\left[1 + \left(\frac{f}{fp}\right)^2\right]} + \frac{f(\varepsilon_1 - \varepsilon_2)}{fs\left[1 + \left(\frac{f}{fs}\right)^2\right]} \quad \text{and} \quad \varepsilon'(f) = \frac{\varepsilon_0 - \varepsilon_1}{\left[1 + \left(\frac{f}{fp}\right)^2\right]} + \frac{(\varepsilon_1 - \varepsilon_2)}{\left[1 + \left(\frac{f}{fs}\right)^2\right]} + \varepsilon_2$$

Here $\varepsilon_0 = 77.6 + 103.3(\theta - 1)$; $\varepsilon_1 = 5.48$; $\varepsilon_2 = 3.51$; $\theta = 300/T$ and T is the ambient temperature (°K). The principal and secondary relaxation frequencies are $f_p = 20.09 - 142(\theta - 1) + 294(\theta - 1)^2$ GHz and $f_s = 590 - 1500(\theta - 1)$ GHz. This specific attenuation when integrated over the vertical path gives the total attenuation in dB. The equation involved is

$$A_c(\text{dB}) = \int_0^{\alpha} \alpha(h)dh \tag{23}$$

Brightness temperatures at different time of different months are made available from the radiometer data where from the total attenuation may be obtained using Eq. (1). Now the measured total attenuation values (A_T) are used to obtain the values of Z_L using the relation (12). Liquid water content may be calculated using Eq. (25). The values of p_L and q_L may be obtained from the radiometric record for the desired period.

6. Analyses and results

Refereeing back to Eq. (10), we see that the term Z_L contains only the vapor part and dry part and can be termed as the attenuation part free from liquid attenuation.

A statistical least square fitting may be adopted between Z_L and calculated values of V obtained by using radiosonde data and the measured values of obtained from radiometer data for the f_1 and f_2 frequency pair. The values from first parenthesis are obtained by substituting the attenuation values by converting the measured radiometric brightness temperature for a pair of frequencies by using Eq. (10). This yield

$$V(\text{kg m}^{-2}) = Z_V p_V + q_V \tag{24}$$

Here, p_V and q_V are the regression coefficients.

Similarly, using Eqs. (12) and (20) we find

$$L(\text{kg m}^{-2}) = Z_L p_L + q_L \tag{25}$$

We have considered the radiometric measurement of the brightness temperature for the 23.834 GHz and 30 GHz pair, as discussed in earlier section. The radiometric outputs in terms of brightness temperature in both the frequency channels were converted to attenuation (dB) by using relation (1). A time series of attenuation values at both the said frequencies have been presented in Fig. 3. It shows that as time passes towards the end of April the attenuation values are going to be decreased and the attenuation at 23.834 is three times larger than those obtained at 30 GHz. The measured values of attenuations for the frequency pair are then substituted in relation (10) to find Z_V. Here it may be noted that the second term in the parenthesis of Eq. (10), is the dry term (A_0) which is mainly due to oxygen present in the ambient atmosphere. This part is calculated by using the MPM model (Liebe, 1985) where the input parameters are only ambient temperature, pressure and humidity of the atmosphere. It was found also that the variation of A_0 is almost negligible over the place in question. But to achieve the good accuracy this part has been included in the present context to get the values of the regression constants like p_V and q_V (see Table 1). The same idea as noted above has been taken into consideration while finding Z_L (see Table 1).

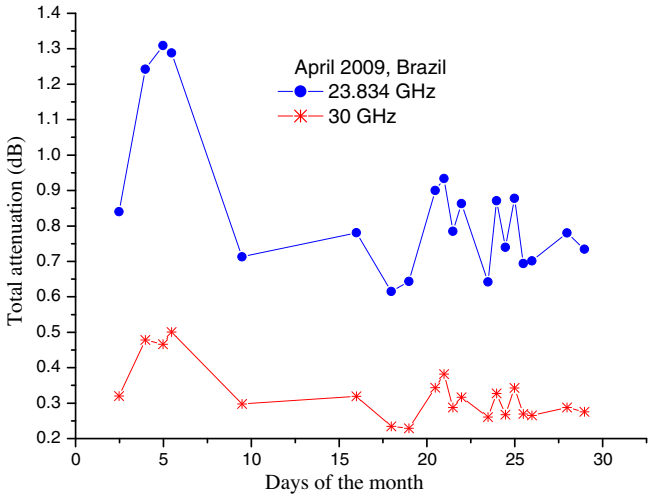

Fig. 3. Time series of attenuation at 23.834 GHz and 30 GHz.

The values of the different regression constants were calculated for the frequency pair (given in Table 1) for the month of April from the multiple regression analyses using radiosonde data. It is to be mentioned that over Brazil the monsoon season prevails from January through April. Now, the regression coefficients for the month of April along with the values of Z_V by exploiting the dual frequency pair have been used for the measured values of integrated water content (kg m^{-2}). A time series of the measured values of vapor content is presented and compared with those obtained by using the radiosonde data (Fig. 4). This shows the vapor content takes maximum in the first half of the month of April (60 kg m^{-2}) and with

Table 1
Different regression constants used in the algorithm.

Regression constants	23.834 GHz and 30 GHz frequency pair
K_1	1.5843
p_V	31.0428
q_V	8.06235
K_2	0.43731
p_L	4.0701
q_L	-2.8409×10^{-4}

Please cite this article in press as: Karmakar, P.K., et al. Radiometric estimation of water vapor content over Brazil. J. Adv. Space Res. (2011), doi:10.1016/j.asr.2011.06.032

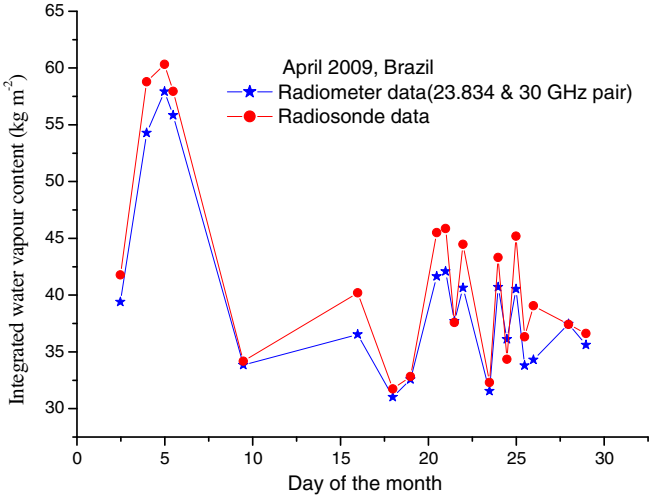

Fig. 4. Time series of integrated water vapor content from radiometer data compared with radiosonde data.

a minimum at the middle of the month (30 kg m^{-2}). An attempt has been made to correlate the measured values of integrated water vapor content with those obtained from the radiosonde data, as shown in Fig. 5. The regression analyses and the line between the radiometric and radiosonde estimation of vapor have been drawn as $V_{\mathrm{RADIOMETER}} = a + bV_{\mathrm{RADIOSONDE}}$, for two different frequency pairs namely (a) 22.234 GHz and 30 GHz pair, (b) 23.034 GHz and 30 GHz pair and (c) 23.834 GHz and 30 GHz pair. While drawing the best fit curve it was found that for the first pair the line fits well with $V_{\mathrm{RADIOMETER}} = A \times V_{\mathrm{RADIOSONDE}}$. The main reason for the choice of two frequency pairs is that the algorithm presented in this text is developed as dual frequency algorithm applicable in the non-rainy condition. Here, although the rainiest month April, 2009 has been chosen, care has been taken to exclude the rainy period data. This has been taken care of by observing the simultaneous data recorded by co-located Disdrometer.

The values of the regression constants are given below:

For 22.234 GHz and 30 GHz pair:
Value of $A = 0.93$; bias $= 4.3$; Standard Deviation $= 2.31$; r.m.s error $= 4.88$.
For 23.034 GHz and 30 GHz pair:
Value of $a = 1.27$, $b = 1.01$; bias $= 3.14$; Standard Deviation $= 1.35$; r.m.s error $= 3.42$.
For 23.834 GHz and 30 GHz pair:
Value of $a = 3.195$, $b = 0.876$; bias $= 2.15$; Standard Deviation $= 1.51$; r.m.s error $= 2.64$.

The bias has been calculated by obeying the relation $\frac{\sum V_{radiometer} - V_{radiosonde}}{number\ of\ data}$ and r.m.s error has been calculated by obeying the relation $\sqrt{bias^2 + sd^2}$.

Now with a view to find out the cloud liquid water content, the relations (11), (12), and (25) have been used. A time series of liquid water content has been plotted (refer to Fig. 6). It is to be noted here that the liquid content goes up to a maximum of 7.0 kg m^{-2} during the month of April. This large value of liquid water content might be due to the presence of thick cloud over the antenna beam. The sudden fall of the graphical presentation is also observed at certain times. It might be due the presence of thin cloud overhead. The thick cloud may be dispersed with time due to wind activity which is happening for a very short period. After this short spell again the accumulation of thick cloud persists which is shown in Fig. 6. If we look back to the work done earlier by Karmakar et al. (2001) then we see that over Kolkata the liquid water content takes a maximum of 1.7 kg m^{-2} and a minimum of less than a kg m^{-2}. But at Brazil the maximum value attains more than 5 kg m^{-2} and a minimum of less than 1 kg m^{-2}.

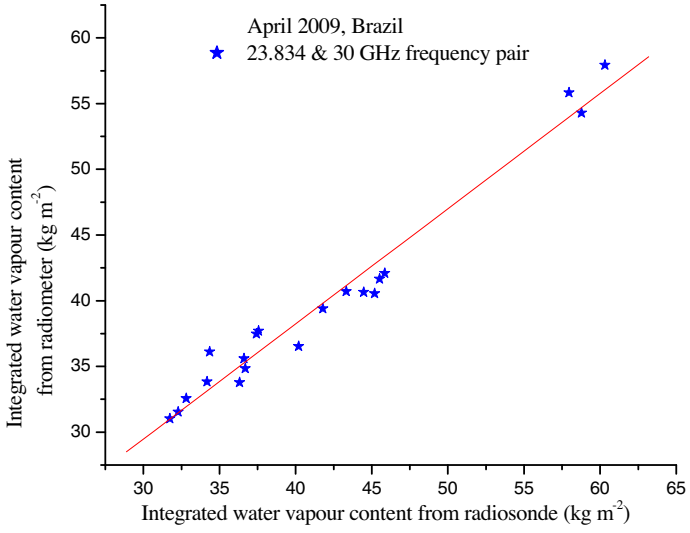

Fig. 5. Correlation between measured and calculated values of vapor content using 23.834 GHz and 30 GHz frequency pair.

Please cite this article in press as: Karmakar, P.K., et al. Radiometric estimation of water vapor content over Brazil. J. Adv. Space Res. (2011), doi:10.1016/j.asr.2011.06.032

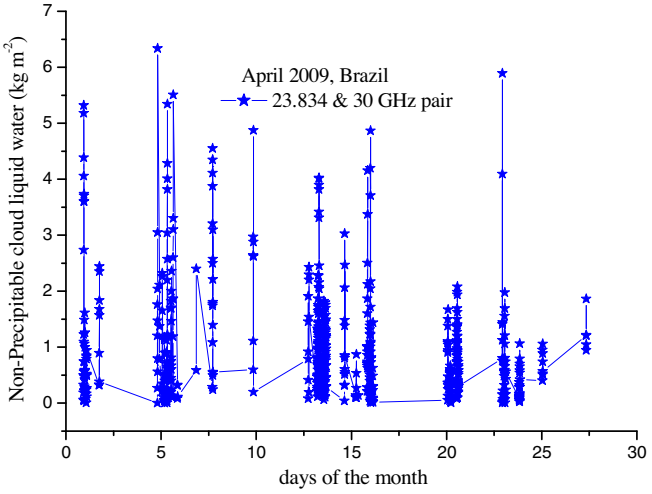

Fig. 6. Time series of cloud liquid water content over Brazil, using 23.834 GHz and 30 GHz frequency pairs.

7. Discussion and conclusion

The regression analysis between the estimated water vapor content by radiometric method and the brightness temperature from our radiometer at 22.234 GHz shows the best linear equations over INPE, Brazil (22°S) as given by Karmakar et al. (2010)

$$W = 478.451T_B + 9574$$

A comparative study between the calculated (using the radiosonde data) values of water vapor content, y and measured (using the radiometer) water vapor content x, has been presented there as

$$y = 0.4218x + 31.31$$

Now taking advantages of latitudinal occupancy of the places of measurement i.e., INPE, Brazil and Institute of Radiophysics and Electronics, Kolkata, (22°N), India, we have presented the same regression analysis over Kolkata (Karmakar et al., 2001) and found as

$$V_m(22.235\ \text{GHz}) = 1.13646\ V\ [\text{percentage error } 5\%]$$
$$(\text{Karmakar etal.,}\ 2001)$$

Here V_m is the measured water vapor content by using 22.235 GHz only and V is the calculated vapor content by using radiosonde data. But the use of dual frequency measurement along with corresponding radiometric data analyses over Kolkata provide the relationship

$$V_m(22.234\ \&\ 31\ \text{GHz}) = 1.0161\ V\ [\text{percentage error } 1.6062\%]$$

So it is worth noting that in estimating water vapor content by using the 22 GHz radiometer data only, the error is 5% while that for measurement of vapor using both 22.235 GHz and 31.4 GHz is 2% relative to the mean. However the liquid water content over Kolkata (22°N), India, were observed as low as 0.02 kg m^{-2} and as high as 1.85 kg m^{-2}.

The measurements of water vapor at Kolkata were done by exploiting 22.235 GHz and 30 GHz pair only. But in the present context, the authors are using two more frequency pairs to get the improved desired accuracy of retrieving vapor at the place of choice. But incidentally, 22.235 GHz is affected by pressure broadening although the resonance peak occurs. Here, the present authors have chosen 23.834 GHz because of its independent nature of pressure broadening to get rid of unwanted signal in the vicinity of 23.834 GHz. Accordingly the accuracy has been improved. Moreover we have used 23.034; a few GHz away from the peak line frequency shows a better result than those obtained by 22.234 GHz.

However the dual frequency measurements of brightness temperatures for getting the vapor and liquid water content have been used since last few decades (Westwater et al., 2005; Hogg et al., 1983; Askne and Westwater, 1986). But because of lack of in situ measurements of cloud liquid, an adequate evaluation of liquid water content over a range of cloud conditions is not available. It is to be mentioned here that radiometric retrievals of humidity up to 10 km height and one-layer cloud liquid sounding have much coarser vertical resolution than radiosonde sounding. The dominant radiosonde error is the representativeness error that results from the characterization of a model cell volume by a point measurement. This type of error is especially important when there are strong temporal or horizontal spatial gradients in the meteorological profiles. Radiometric retrievals can be temporally averaged and, in these strong gradient (temporal or horizontal) conditions may be less susceptible to representativeness error than radiosonde soundings. One of the potential advantages of high-temporal-resolution radiometric data (5–15 min) is that the data could be directly assimilated into weather forecast models to improve short term forecasts.

Acknowledgements

We thank CNPq PCI programme for partial support of this research (Proc. 680002/2007 – 3).

References

Allnutt, A.L. Slant path attenuation and space diversity results using 116 GHz radiometers. Proc. IEE 123, 1197–1200, 1976.

Askne, J., Westwater, E.R. A review of ground-based remote sensing of temperature and moisture by passive microwave radiometers. IEEE Trans. Geosci. Remote Sens., 340–352, 1986.

Cimini, D., Westwater, E.R., Gasiewski, A.J., Klein, M., Leuski, V., Liljegren, J.C. Ground-based millimeter and submillimeter-wave observations of low vapor and liquid water contents. IEEE Trans. Geosci. Remote Sens., 45, 2169–2180, 2007.

David, K. Adams, Rui, M.S., Fernandes, E.R., Maia, J.M., Sapucci, L.F., Machado, L.A.T., Icaro Vitorello, Jo~ao Francisco Galera Monico, Kirk, L.H., Gutman, S.I., Naziano Filizola, Richard, A. Bennett. A dense GNSS meteorological network for observing deep convection in the Amazon. Atmos. Sci. Lett. 312, 2011, doi:10.1002/asl. Published online in Wiley Online Library (wiley on line library.com).

Evans, J.V., Hagfors, T. Radio Astronomy. Mc-Graw Hill Book Co., Inc. New York, 1968.

Grody, C. Remote sensing of atmospheric water content from satellite using microwave radiometry. IEEE Trans. Antennas and Propagation 24, 155–162, 1976.

Hogg, D.C., Guiraud, F.O., Sinder, J.B., Decker, M.T., Westwater, E.R. A Steerable dual-channel microwave for measurement of water vapor and liquid in the troposphere. J. Climate Appl. Meteorol. 22, 789–806, 1983.

Janssen, M.A. A new instrument for the determination of radiopath delay due to atmospheric water vapor. IEEE Trans. Geo Sc. and Remote Sensing 23, 455–490, 1985.

Karmakar, P.K., Chattopadhaya, S., Sen, A.K. Estimates of water vapor absorption over Calcutta at 22.234 GHz. Int. J. Remote Sensing 20 (13), 2637–2651, 1999.

Karmakar, P.K., Rahaman, M., Sen, A.K. Measurement of atmospheric water vapour content over tropical location by dual frequency microwave radiometry. Int. J. Remote Sens. 22, 3309–3322, 2001.

Karmakar, P.K., Maiti, M., Calheiros, A.J.P., Angelis, C.F., Machado, L.A.T., Da Costa, S.S. Ground based single frequency microwave radiometric measurement of water vapour. Int. J. Remote Sens. 11, in press, doi:10.1080/01431161.2010.543185.

Liebe, H.J. An updated model for millimeter wave propagation in moist air. Radio Science 20, 1069–1089, 1985.

Maitra, A., Chakraborty, S. Cloud liquid water content and cloud attenuation studies with radiosonde data at a tropical location. J. Infrared Milli Terahz Waves 30, 367–373, 2009.

Moran, J.M., Rosen, B.R. Estimation of propagation delay through troposphere and microwave radiometer data. Radio Science 16, 235–244, 1981.

Pandey Prem, C., Gohil, B.S., Hariharan, T.A. A two frequency algorithm differential technique for retrieving precipitable water from satellite microwave radiometer (SAMIR-II) on board Bhaskara II. IEEE Trans. Geo Sc. and Remote Sensing 22, 647–655, 1984.

Resch, G.M. Another look at the optimum frequencies for water vapour radiometer, TDA progress report, 1983.

Salonen, E. New prediction method of cloud attenuation. Electron. Lett. 27, 1106–1108, 1991.

Sherwood, S.C., Roca, R., Weckwerth, T.M., Andronova, N.G. Tropospheric water vapour convection and climate: a critical review. Rev. Geophys. 48, RG2001, doi:10.1029/2009RG000301, 2009.

Simpson, P.M., Brand, E.C., Wrench, C.L. Liquid water path algorithm development and accuracy. Microwave radiometer measurements at Chilbolton. Radio Communications Research Unit CLRC-Rutherford Appleton Laboratory Chilton, DIDCOT, Oxon. OX11 0QX, UK, 2002.

Ulaby, F.T., Moore, R.K., Fung, A.K.. Microwave remote Sensing Active and Passive, vol. 1. Artech House, Norwood, 1986.

Westwater, E.R. Ground based determination of low altitude temperature profiles by microwaves. Monthly weather Review 100 (1), 15–28, 1972.

Westwater, E.R. The accuracy of water vapor and cloud liquid determination by dual-frequency ground-based microwave radiometry. Radio Science 13, 677–685, 1978.

Westwater, E.R., Guiraud, F.O. Ground-based microwave radiometric retrieval of precipitable water vapor in the presence of clouds with high liquid content. Radio Science 13, 947–957, 1980.

Westwater, E.R., Crewell, S., Mätzler, C., Cimini, D. Principles of surface-based microwave and millimeter wave radiometric remote sensing of the troposphere. quaderni della società italiana di elettromagnetismo 1, 3, 2005.

Please cite this article in press as: Karmakar, P.K., et al. Radiometric estimation of water vapor content over Brazil. J. Adv. Space Res. (2011), doi:10.1016/j.asr.2011.06.032

ANEXO 10

DESENVOLVIMENTO

DESTAQUE

Análises de incertezas foram feitas para as projeções dos modelos globais do IPCC AR4 e para as projeções regionais derivadas do modelo (regional) Eta do CPTEC, para a América do Sul. Uma campanha de campo foi realizada em março de 2010, em Alcântara, Maranhão, nordeste do Brasil (Projeto CHUVA), com o objetivo de estimar as incertezas em simulações de chuva. Os dados produzidos foram posteriormente assimilados nos modelos globais e regionais do CPTEC.

PRINCIPAIS PERGUNTAS DE PESQUISA

Como podem ser estimadas as incertezas nas projeções de clima futuro geradas pelos modelos globais e regionais?

Como podem ser reduzidas as incertezas em processos importantes como as simulações/projeções de chuva?

PALAVRAS-CHAVE

Projeções de mudanças climáticas, analise de incertezas, campanha de campo, modelos climáticos regionais, modelos climáticos globais, microfísica de nuvens.

Cenários Climáticos Futuros e Redução de Incertezas

Duas abordagens para a análise de incerteza estão sendo utilizadas: (1) a primeira envolve a estimativa de incertezas em conjuntos de projeções do modelo gobal HadCM3 do Hadley Centre do UK Met Office, para o cenário de emissões A1B. Fazendo uso do método de Conjunto de Perturbações Físicas (*Perturbed Physics Ensemble,* PPE), quatro membros do modelo HadCM3 têm sido utilizados como condições de contorno para o modelo regional Eta-CPTEC, e as projeções para 2010-2100 foram extraídas desse refinamento da escala espacial. Primeiro, o método PPE é aplicado para avaliar as incertezas no nível das bacias hidrográficas (São Francisco, Amazonas e Paraná), em seguida é aplicado a cada ponto de grade em toda a América do Sul. (2) A segunda abordagem considera as análises de incerteza nas observações de precipitação, que são utilizadas para avaliar tendências de longo prazo, bem como as incertezas na simulação da precipitação a partir de modelos gobais e regionais do clima. A introdução dos processos de física de nuvens na modelagem reduz erros nas simulações de chuva nos modelos climáticos. Estimativas melhoradas de chuva a partir de dados de satélite permitem o estudo de possíveis alterações nos regimes de chuvas com maior precisão. A fim de alcançar este objetivo, medições de precipitação in loco realizadas durante a experiência de campo do Projeto CHUVA serão utilizadas para auxiliar a compreensão dos processos físicos nas nuvens. Isto possibilitará melhorar a calibração da chuva além de uma melhor descrição da microfísica das nuvens nos modelos que a contém, o que possibilitará a geração de projeções mais realistas de chuva futura.

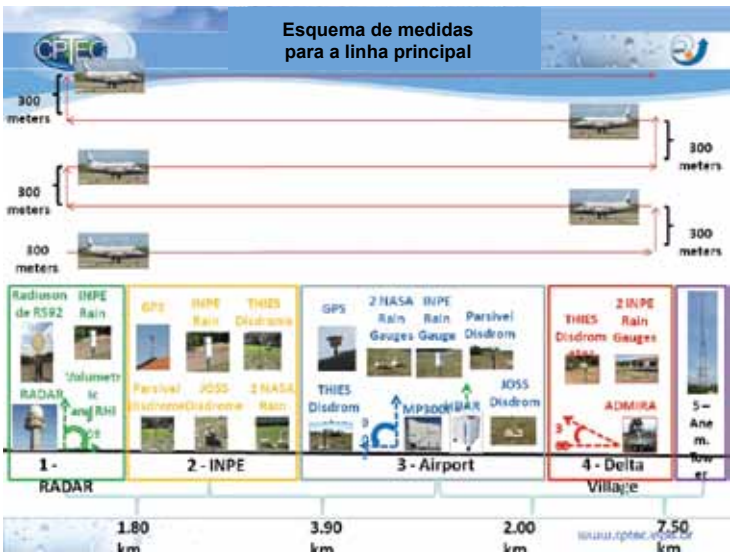

Estratégia de medição da campanha de campo CHUVA

COORDENADORES

JOSÉ A. MARENGO E
LUIZ A. T. MACHADO

INPE, São José dos Campos, SP, Brasil

jose.marengo@inpe.br
luiz.machado@cptec.inpe.br

FORMAÇÃO DE RECURSOS HUMANOS

Oito estudantes de doutorado estão envolvidos com as campanhas de campo e várias vagas de pós-doutorado estão sendo abertas para o trabalho de análise dos dados produzidos na campanha do Projeto CHUVA. Dois estudantes de doutorado estão trabalhando em colaboração com pesquisadores do UK Met Office na implementação do método de EPP para projeções de mudanças climáticas.

PRINCIPAIS EVENTOS

Em dezembro de 2009 organizou-se uma reunião geral envolvendo todos os participantes do INCT para Mudanças Climáticas, do CPTEC e do Centro de Ciências do Sistema Terrestre do INPE (CCST/INPE). Sessões especiais foram realizadas na Reunião Anual da Associação de Geofísica dos EUA (American Geophysical Union – AGU), em Foz do Iguaçu, Paraná, e na Segunda Conferência Internacional do Clima e Desenvolvimento Sustentável em Regiões Semi-Áridas, realizada em Fortaleza, Ceará, em 2010.

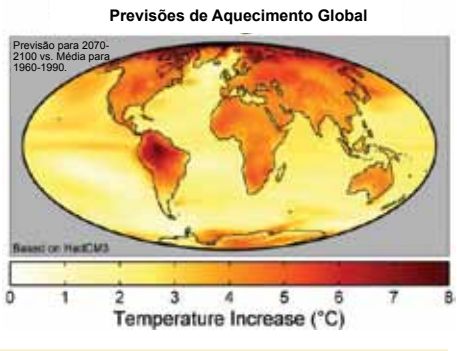

Destaques Científicos

Os novos cenários climáticos regionais já estão sendo utilizados por vários grupos do INCT para Mudanças Climáticas, da Rede CLIMA e por outros grupos de pesquisa das universidades e institutos federais, envolvidos principalmente com análises de impacto e avaliações de vulnerabilidade. Estas atividades fazem parte dos esforços para preparar a 2ª Comunicação Nacional para a Convenção-Quadro das Nações Unidas para Mudança Climática *(2nd National Communication of Brazil to the United National Framework Convention on Climate Change Convention - UNFCCC).* Este subprojeto trabalha no desenvolvimento de uma versão melhorada do modelo regional ETA do CPTEC que inclui a mudança nas concentrações dos GEE e no esquema de vegetação dinâmica (resolução de 20 ou 40 km), forçada por vários modelos globais do clima e para vários cenários de emissões até 2100. Isto mostra as sinergias com o subprojeto do Modelo Brasileiro do Sistema Climático Global (MBSCG), que está gerando cenários de mudanças climáticas para o Brasil e para a América Latina. O modelo regional Eta do CPTEC também será rodado com as projeções globais do MBSCG como condições de contorno. O segundo componente irá realizar experimentos de campo em sete locais para investigar os diferentes regimes de precipitação no Brasil. Ele pretende aumentar o conhecimento dos processos de nuvens, a fim de reduzir as incertezas nas estimativas de precipitação, principalmente nas de precipitação de nuvens quentes e, desta forma, melhorar o conhecimento do balanço de água e de energia.

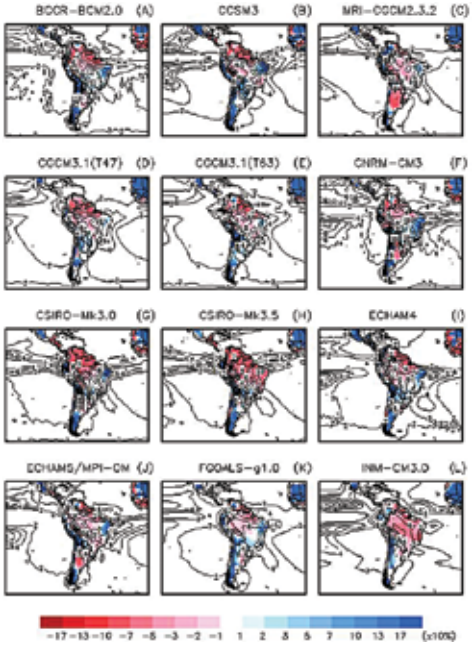

Climatologia para o verão austral (Dezembro-Fevereiro) simulada pelos 12 modelos globais do IPCC AR4 para 1901-1998. Contornos (a cada 2 mm/dia) representam a chuva atual e as cores representam o viés do modelo (simulado menos observado, x10%).

INTERFACE CIÊNCIA-POLÍTICAS PÚBLICAS

O trabalho utilizando cenários futuros de mudança climática para estimar os impactos e a vulnerabilidade a ela inclui vários setores, como agricultura, recursos hídricos, biodiversidade, saúde humana, regiões semi-áridas, turismo e zonas costeiras. Os cenários de mudanças climáticas para Brasil e América Latina serão apresentados na forma de relatórios nacionais ou regionais e mapas temáticos georreferenciados, de modo que os efeitos adversos da mudança do clima a curto, médio e longo prazo possam ser identificados e os governos possam decidir sobre as medidas e opções de adaptação.

PUBLICAÇÕES SELECIONADAS

Diedhiou A, Machado LAT, Laurent H. Mean Kinematic Characteristics of Synoptic Easterly Disturbances over the Atlantic. Advances in Atmospheric Sciences, v. 27, p. 1-17, 2010.

Marengo JA, Chou SC, Kay G, Alves LM, Pesquero JF, Soares WR, Santos DC, Lyra AA, Sueiro G, Betts R, Chagas DJ, Gomes JL, Bustamante JF & Tavares PD. Development of regional future climate change scenarios in South America using the Eta CPTEC/HadCM3 climate change projections: Climatology and regional analyses for the Amazon, São Francisco and the Parana River Basins. Accepted, Climate Dynamics.

ANEXO 11

Cover Sheet - DRAFT 9 August 2011

Proposal Title

- "Intensive Ground-Based Research in Amazonia 2014" (IGRA-2014)

Research Sites for Proposed Activities

- T0: Atmospheric Tall Tower Observatory (ATTO) (-2.147°S, -59.005°W)
- T1: Inside Manaus (INPA/UEA) (-3.097°S, -59.987°W)
- T2: Downwind Margin of Manaus (ca. -3.2°S, -60.1°W)
- T3: ARM Mobility Facility (AMF) (-3.213°S, -60.599°W)
- FT3: Flux Tower nearby T3-AMF (ca. -3.213°S, -60.599°W)
- K34: Flux Tower (54 m) (-2.609°S, -60.209°W, 50 km north of Manaus)
- K67: Flux Tower (65 m) (-2.855°S, -54.959°W) (nearby Santarem)
- SGC: Flux Tower (ca. 0.48°N, -66.5°W) (nearby São Gabriel da Cachoeira)

Date of Proposed Activities

- 1 June 2012 until 31 May 2015
    - Intensive operations during 3 months of wet season and 3 months of dry season in 2014
    - Baseline measurements and ongoing monitoring from 2012 to 2015 at several site locations so that intensive measurements can be put into context of annual and seasonal variability

One-Sentence Scientific Synopsis

- The proposed scientific project and observations have the focus of *understanding and quantifying the influence of aerosol and gaseous outflow from a tropical megacity on the carbon cycle, the cloud life cycle, the aerosol life cycle, and the cloud-aerosol-precipitation interactions*, including as a baseline the functioning of each cycle and their couplings for pristine conditions.

Background and Motivation

The carbon, water, and energy flows in the Amazon Basin are important not only as primary engines affecting ecosystem and climate functioning of the Southern Hemisphere but more broadly for the planet. Any accurate climate model must succeed in a good description of the Basin, both in its natural state and in states perturbed by regional and global human activities. At the present time, however, tropical deep convection in a natural state is poorly understood and modeled, with insufficient observational data sets for model constraint. Furthermore, future climate scenarios resulting from human activities globally show the possible drying and the eventual possible conversion of rain forest to savanna in response to global climate change. Based on our current state of knowledge, the governing conditions of this catastrophic change are not well defined. Human activities locally, including the economic development activities that are growing the population and the industry within the Basin, also have the potential to shift regional climate, most immediately by an increment in aerosol number and mass concentrations, and the shift is across the range of values to which cloud properties are most sensitive. For example, natural conditions of 300 particles cm^{-3} prevail in much of the Amazon Basin during the pristine wet season and cloud properties are most sensitive to shifts from 300 to 1000 cm^{-3}; polluted regions of the world have concentrations that are much greater than 1000 cm^{-3}. Moreover, Amazon forests are potentially susceptible to climate change, and can influence the course of climate change through complex, non-linear feedback processes. Amazonia holds vast reserves of organic carbon in an extremely dynamic ecosystem, mediating enormous fluxes of CO_2, H_2O, fixed nitrogen, and highly reactive organic species (Biogenic Volatile Organic Carbon, "BVOCs"). The ecosystem provides the fuel for vast fires that release carbon and modify atmospheric radiation, precipitation, and composition regionally and globally. Amazonia provides the free radical precursors that drive the most vigorous photochemistry on Earth and, through deep convective inputs, the most important reactive species in the climatically crucial regions of the Tropical Tropopause Layer (TTL) and lower tropical stratosphere.

The convective activity and the atmospheric circulation of tropical South America are part of an American monsoon system.[1] Any changes in tropical precipitation can have significant, potentially global consequences because of non-linear interactions of tropical waves with precipitation in the Amazon, leading also to possible changes in the tropical Atlantic intertropical convergence zone (ITCZ).[2] The effects of aerosol particles on cloud microphysical properties, cloud cover, precipitation, and regional climate over the Amazon are significant, yet the region has been the focus of relatively little research compared to other parts of the world and especially compared to its importance. The region may be particularly susceptible to changes in aerosol particles because of the low background concentrations and high water vapor levels, indicating a regime of cloud properties that is highly sensitivity to aerosols. Aerosol concentrations are rapidly changing with deforestation and the associated biomass burning and economic development. Although deforestation rates had been declining during the last 5 years, preliminary data for the period of 2010-2011 shows a recent increase. The climatic implications for strong aerosol-cloud dynamic interaction are profound,[3-6] ranging from modulation of local precipitation intensity to modifying large-scale circulations and energy transport associated with deep convective regimes (e.g., Hadley or Walker circulation). Suppression of rainfall can potentially lead to a positive feedback through a drier land surface, stronger susceptibility to fires and even greater aerosol-induced suppression of rainfall.[7] Preliminary studies indicate that higher concentrations of aerosol particles might increase the intensity of precipitation in the Amazon

region.[8,9] Research progress requires data and observations, hence, the motivation for "Intensive Ground-Based Research in Amazonia 2014" (IGRA-2014).

In the wet season, the Amazon Basin is one of the most pristine locations on Earth for continental aerosols. These aerosols are in dynamic balance with the ecosystem (which produces them) and the hydrologic cycle (which removes them). Manaus, a city of nearly 2 million people, is an isolated urban area within the otherwise pristine Amazon Basin. The city's electricity is produced by burning high-sulfur fuel oil as well as by hydroelectric power (Balbina). The city is growing very fast in both population and areal extent, and the incremental energy needs are being met mainly by fossil-fuel power plants. A major bridge completed in 2011 between Manaus and Iranduba will connect an industrial region with the city and certainly increase the production of goods that may contribute to the aerosols and pollution. The plume from the city has high concentrations of SO_2, NO_x, and soot, among other pollutants. The proposed deployment will enable the study of how aerosol and cloud life cycles, including cloud-aerosol-precipitation interactions are influenced by pollutant outflow from a tropical megacity. This study, in addition to understanding the present-day effects of a tropical megacity on a pristine environment, will also provide important information for broader applications into thinking about possible future changes of climate planet wide: human activities by the year 2050 are projected to greatly increase the megacity count worldwide, particularly in tropical regions like the city of Manaus.

The large societal need is an understanding of how perturbations of the inputs into the natural system result in changed clouds, radiative balance, climate, and feedbacks among them. The prevailing regime of aerosol-cloud interaction in the natural environment of the Amazon Basin is distinctly different from polluted continental regions,[10] where particle concentrations are orders of magnitude higher. So far, however, the effects of urban outflow in modifying CCN properties of a pristine tropical rain forest have not been investigated. The existence of an isolated plume in an otherwise very pristine environment downwind of Manaus offers the possibility to investigate the evolution of the aerosols over several hours following emission. Changes in CCN properties, both because of changes in chemical composition and changes in number-size distributions, can have important effects on the cloud life cycle, precipitation and climate.

The IARA-2014 project is part of an umbrella research effort called Observations and Modeling of the Green Ocean Amazon (GoAmazon2014) that is organized under the aegis of the Brazil-led Large-Scale Biosphere Atmosphere Experiment in Amazonia (LBA). GoAmazon2014 is organized into three main pieces:

(1) the baseline project (i.e., entitled "ARM Mobility Facility" (AMF2014)) that runs continuously for 12 months and is situated for the most part at a pasture site near Manacapuru;

(2) the airborne intensive operating period (entitled "Intensive Airborne Research in Amazonia 2014" (IARA2014)) that takes place in focused periods of the wet and dry seasons and be based out of the Manaus Eduardo Gomes International Airport; and

(3) the ground-based intensive operating period (i.e., this proposal) (IGRA2014) that takes place in focused periods of the wet and dry seasons and that spans multiple fixed sites including T0-ATTO, T1-UEA/INPA, T2-TBD, T3-AMF, and K34.

These three projects AMF2014, IARA2014, and IGRA2014 are administered under separate scientific expedition licenses so that uncertainties and contingencies within each do not

jeopardize the integrity of umbrella research effort of GoAmazon2014. The three projects differ significantly in time and geographic scopes and therefore in partnerships, funding, and permissions.

Scientific Objectives

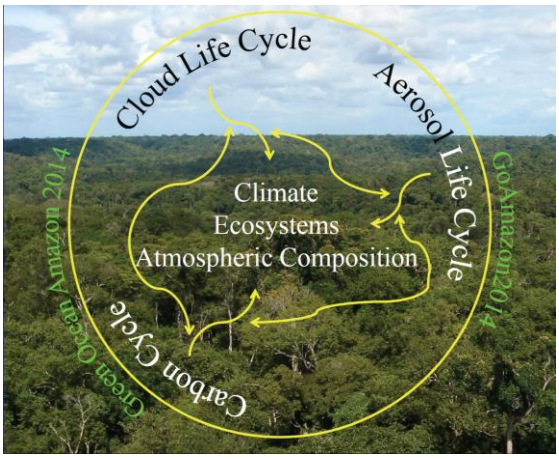

The scientific objectives of the project that can be broadly categorized as related to the Carbon Cycle, the Aerosol Life Cycle, the Cloud Life Cycle, and Aerosol-Cloud-Precipitation Interactions. Detailed objectives within each of these broad categories are as follows:

Carbon Cycle - improve Community Earth System Model (CESM) for land-atmosphere processes in the Amazon Basin, including aerosol-cloud-precipitation connections

1. Reduce uncertainties in our knowledge of feedbacks between vegetation-hydrology that underlie the Amazon forest dieback hypothesis.[11,12] The uncertain range of feedbacks at present leads to large differences in ESM predictions;
2. Response of photosynthesis and transpiration, including BVOC emissions, to changes in the direct and diffuse components of incoming solar radiation,[13,14] i.e., in the context of current and future scenarios of aerosols and clouds in the Amazon Basin; and
3. Implicit in foci 1 to 2 is the quantification of the effect of pollution on the flows of carbon through the ecosystem and the interconnections between the ecosystem and climate and atmospheric composition.

Aerosol Life Cycle - accurate modeling of aerosol sources/sinks and aerosol optical, CCN, and IN properties, as affected by pollution of pristine tropical environments

1. The interactions of the urban pollution plume with biogenic volatile organic compounds in the tropics, especially the impact on the production of secondary organic aerosol, the formation of new particles, and biogenic emissions of aerosols and their precursors;
2. Influence of anthropogenic activities on aerosol microphysical, optical, cloud condensation nuclei (CCN), and ice nuclei (IN) properties in the tropics; and
3. Implicit in foci 1 to 2 is the quantification of aerosol optical and CCN properties in perturbed and unperturbed air masses.

Cloud Life Cycle - development of a knowledge base to improve tropical cloud representation parameterizations in regional and global circulation models (GCMs)

1. The transition from shallow to deep cumulus convection during the daily cycle of the Amazon Basin, with comparison and understanding to other environments;
2. The role of landscape heterogeneity—the Manaus urban area as well as the 10-km-scale of river width—on the dynamics of convection and clouds (+carbon cycle);
3. The evolution of convective intensity from severe storms in the dry season to moderate storms in the wet season;
4. Connections between the cloud life cycle and the cross-atmosphere radiation budget; and

5. Implicit in foci 1 through 4 is the development of a knowledge base and test cases that will improve tropical cloud parameterizations in global climate models (GCMs).

Cloud-Aerosol-Precipitation Interactions - improvement of parameterizations of aerosol-cloud interactions in climate models

1. Aerosol effects on deep convective clouds, precipitation, and lightning under different aerosol and synoptic regimes, including the roles of aerosols in changing regional climate and atmospheric circulation; and
2. Data-driven improvement of parameterizations of aerosol-cloud interactions in the climate models.

The theme uniting these objectives is the development of a data-driven knowledge base for predicting how the present-day functioning of energy, carbon, and chemical flows in the Basin might change, both due to external forcing on the Basin from global climate change and internal forcing from past and projected demographic changes in the Basin. The ultimate goal is to estimate future changes in direct and indirect radiative forcing, energy distributions, regional climate, ecosystem functioning, and feedbacks to global climate. In this regard, the presented objectives are representative, and further definition and broadening can be expected as the science team spins up prior to deployment.

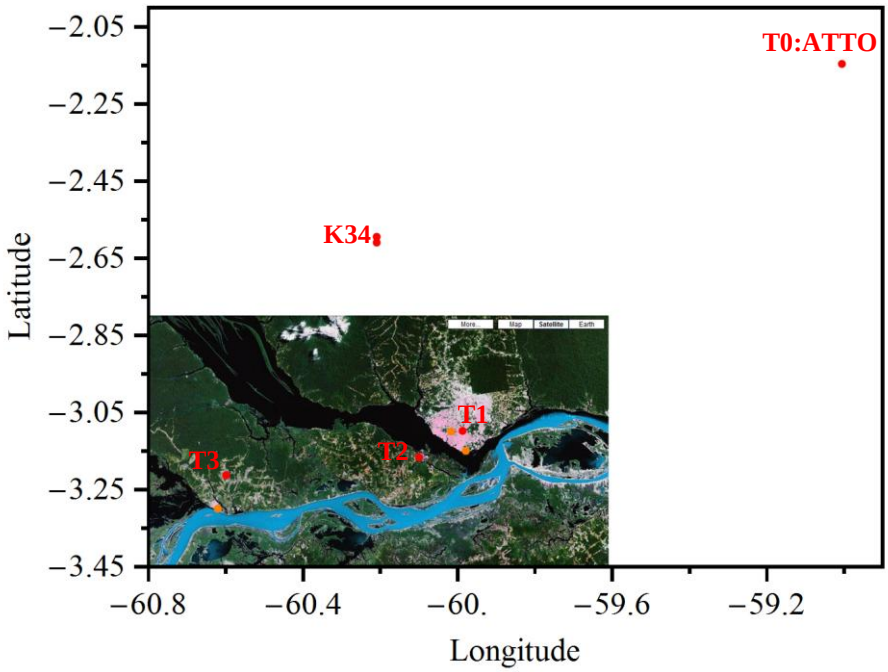

Figure 1. Map of site locations in and around Manaus, including a highlight of ground cover between Manaus and Manacapuru. The T3 site is 70 km downwind of Manaus, corresponding to 2 to 6 hr of advection time for typical winds at 1 km altitude.

Measurement Strategy

To address the proposal's scientific objectives, we propose to deploy at multiple sites during (1) intensive operating periods in the wet and dry seasons of 2014 as well as (2) lower intensity activities from 1 June 2012 through 31 May 2015 to provide information on the annual and seasonal variability at these sites (Figure 1)**.** In this way, the wide range of measurements during the intensive operating periods can be understood within a larger context. The intensive operating periods are timed to overlap with the deployment of the G1 aircraft (cf. IARA-2014 document).

The urban plume of Manaus passes westward toward Manacapuru into the center of the Amazon Basin. The plume downwind greatly influences aerosol production and radiative balance (Figure 2). Kuhn et al.[15] reported on the impact of the pollution plume of Manaus in the central Amazonia on aerosol concentrations, the oxidant cycle, and other measures of air quality on the otherwise pristine conditions of the central Amazon Basin. In this unique scientific environment, sampling inside and outside of the plume can unambiguously unravel the influence of human activities on tropical atmospheric chemistry and drivers of climate. The unique aerosol types in the different seasons provide an excellent opportunity to investigate how different aerosol compositions affect the CCN population and the consequent influence on cloud properties and precipitation. The wet season provides some of the most pristine continental conditions on Earth (Figure 3). The dry season permits investigation of the influence of biomass burning, which

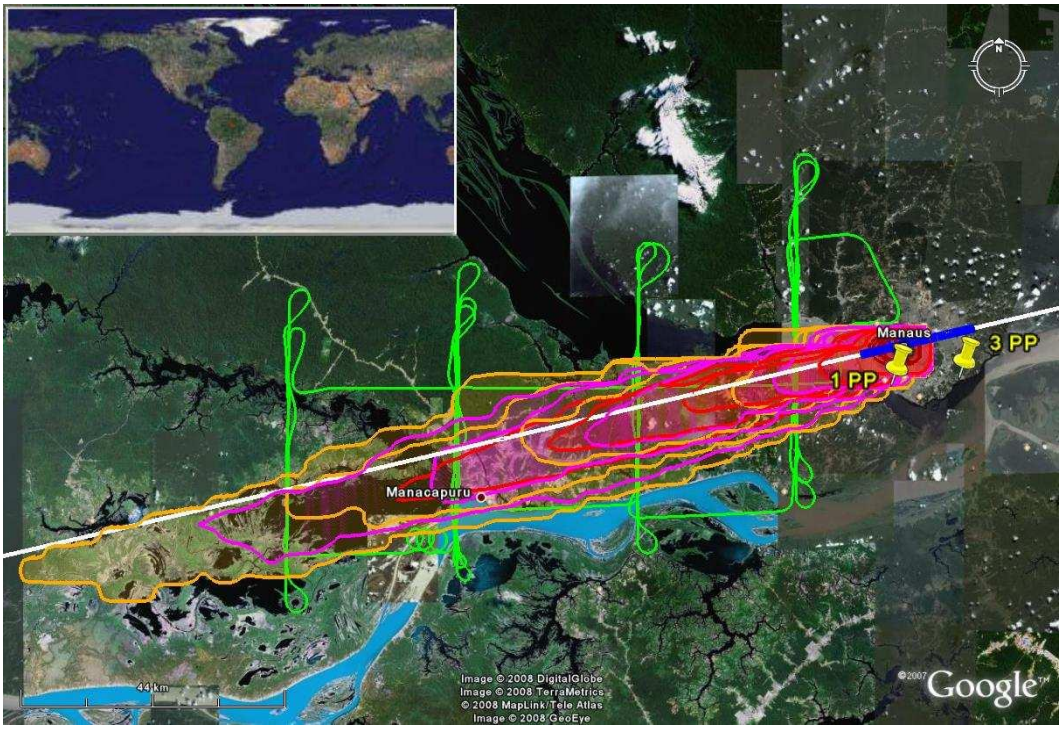

Figure 2. Land cover image (GOOGLE EARTH) with an overlay of a flight pattern on 19 July 2001 from 10.00-14:00 (local time) that samples the Manaus plume. Flight track GPS data are shown in green line. The output of a HYSPLIT dispersion model run from the Manaus plume is indicated by the red/orange contour lines. The two yellow pins indicate the locations of power plants (3 PP, 560 MW capacity; 1 PP, 125 MW). Figure is adapted from Kuhn et al.[15] Kuhn et al.[15] transected the urban plume of Manaus in a lagrangian fashion at 10, 40, 70, and 100 km downwind. The Manaus plume is well defined because of persistent easterly winds throughout the year. The width of the urban plume was about 20-25 km, resembling the dimension of the city itself, with little downwind spreading, i.e., there was distinct clean air on both sides of the pollution plume.

ranges from a dominating perturbation at the southern edge of the Amazon Basin to a more diffuse elevation of background pollution in the central part of the Basin near Manaus.

The biosphere and atmosphere are at once both causes and effects of myriad processes of one on the other, especially in the natural Amazon Basin. Every carbon atom and every water molecule cycle through both the biosphere and the atmosphere in this environment. For this reason, any comprehensive understanding and accurate future predictions of the Amazon Basin, especially in the context of future implementation and improvements to the CESM, must include connections among ecosystem stressors and climate impacts. A study of **the carbon cycle** is therefore an important focus of IGRA2014.

A major mechanism the biosphere-atmosphere connection is tied to the factors influencing the emissions of biogenic volatile organic compounds (BVOCs). The coupling between the carbon and hydrological cycle, as mediated by plants, is that BVOCs are oxidized in the atmosphere to form low vapor-pressure oxygenated products that condense into the particle phase. In the climate-relevant submicron size regime, 90% of the particle mass concentration can be traced back to this secondary organic material produced by the oxidation of BVOCs. This submicron organic material is then the dominant contribution to cloud condensation nuclei. Cloud formation in the Amazon Basin is in a regime high sensitivity to CCN number concentrations and chemistry because the of the low CCN number concentration. Poeschl et al., however, offered evidence for rainforest aerosols as biogenic nuclei of clouds and precipitation in the Amazon. For this rubric a linear sequence exists linking terrestrial ecosystems to climate, as follows: {plants,stressors} → BVOC emissions → atmospheric oxidation → particle formation → CCN → clouds → rainfall. The proposed project will fill the gaps both qualitatively with respect to important processes as well as quantitatively with respect to values of important parameters. Another goal of the proposed project is to understand the connections of those changed aerosol and CCN properties on altering radiation and the effects of that altered radiation quality on plants. In this way, an integrated understanding both of the forward connection of ecosystem on climate, as well as the backward connection of climate on ecosystem, can be developed within the scope of this project.

In regard to experimental strategy, terrestrial ecosystem studies require multiyear observations as well as a diversity of observation locations. Given these requirements, IGRA2014 is described as having a component of lower intensity activities from 1 June 2012 through 31 May 2015, which are largely geared toward tie-ins to the carbon cycle. Intensive operating periods in 2014 will focus on the connections of the carbon cycle to the other physicochemical aspects of IGRA2014

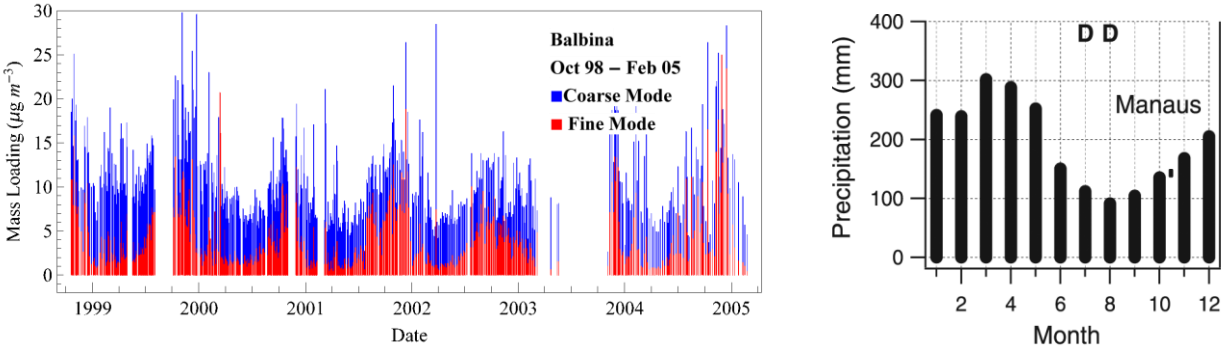

Figure 3. (left column) Time series of particle mass concentrations in Balbina. Data are shown as stack bar plots of fine (red; < 2 μm) and coarse (blue; 2 to 10 μm) size fractions. Adapted and updated from Artaxo et al.[16]
(right column). Seasonal variation of the rainfall in Manaus. Symbol "D" indicates dry season, as defined using high cloud cover. Adapted from Machado et al.[17]

(i.e., aerosol life cycle, cloud life cycle, and aerosol-cloud-precipitation interactions). The other requirement of diversity of locations is represented by movement from the eastern side of the Basin (K67), to the central region of the basin (K34), to the western side of the Basin (SGC). There is a gradient of increasing rainfall and decreasing Atlantic influence along this line; a wet-dry season contrast is strong at K67, intermediate at K34, and almost entirely absent at SGC. These sites will set the baseline for understanding the natural operation of the carbon cycle within the Basin, specifically with respect to tie-in questions of radiation quality as well as BVOC emissions that are the focus of the intensive operating periods of IGRA2014. The Amazon Basin is heterogeneous in many respects, and multiple sampling sites are important. With the context of natural functioning in place across multiple years and seasons, the tower at FT3 nearby the AMF facility will focus on the perturbations to natural functioning induced by pollution.

In addition to altered radiation, changes in nutrient cycles in the downwind plume of Manaus are important in ecosystem functioning. For instance, the atmospheric NO_x concentration increases 1000-fold and there is a corresponding increase in dry deposition. The effect of nitrogen fertilization on tropical forests is a topic of active research[18-20] that is proposed for investigation in IGRA2014. These new data are broadly relevant to the future of the Amazon Basin, which under many scenarios is linked to economic development. Development brings transportation, which is a source of NO_x and soot. Brazil is also attempting to re-balance its energy portfolio with less dependence on hydropower and a greater mix of fossil fuels, bringing along greater emissions of NO_x. The atmospheric oxidant cycle in the Basin at present is in a regime of dominant HO_2 chemistry because NO_x concentrations are on the order of 100 ppt. Economic development can be expected to greatly increase the NO_x concentrations and therefore influence the atmospheric oxidant cycle. This cycle is responsible for the oxidation of BVOCs that eventually form CCN. The regulation of the hydrological by the current gaia stasis can be disrupted: isoprene is the dominant BVOC emitted in the Amazon and under higher NO_x conditions this BVOC forms considerably less particle-phase organic material, favoring instead higher-vapor pressure products. The associated implications on rainfall patterns are yet to be defined. These aspects will be investigated in an integrated manner by allied studies on the aerosol life cycle, as part of IGRA2014.

In relation to the natural functioning of the **aerosol life cycle** in the Amazon Basin, Chen et al.[21] characterized submicron atmospheric particles using an Aerodyne high-resolution aerosol mass spectrometer (AMS) during the wet season of 2008 in an unpolluted site north of Manaus. Patterns in the mass spectra closely resembled those of secondary-organic aerosol particles formed in environmental chambers from biogenic precursor gases. High-resolution mass spectra of model SOA particles (obtained in the Harvard Environmental Chamber) can be linearly combined to largely reproduce the patterns observed in AMAZE-08 (unpublished data). The organic mass concentration of the Amazonian ecosystem had an average value of 0.6 $\mu g\ m^{-3}$ and an average elemental oxygen-to-carbon (O:C) ratio of 0.42. This average O:C ratio is also similar to that of laboratory SOA particles at realistically-low precursor concentrations (e.g., 0.40 to 0.45 in Shilling et al.[22]). For comparison, urban-combustion primary emissions (O:C < 0.10) and aged regional particles (O:C ≈ 0.9) observed near Mexico City had significantly different values.[23] The influence of the pollution outflow of Manaus on formation of SOA, notably its mass loading and size distribution, as well as its radiative, hygroscopic, and CCN properties, is proposed for investigation as part of IGRA2014.

A particular focus is the interaction of biogenic and anthropogenic emissions and their effect on SOA formation. The larger part of VOC emission is biogenic, yet a complex interaction of anthropogenic and biogenic emissions must be investigated. Studies suggest small amounts of anthropogenic emission can trigger large changes in the dominant chemical pathways that guide the conversion of biogenic VOCs into the production of SOA. Global datasets of organic aerosol measurements juxtaposed to chemical transport model simulations suggest that the enhancement of SOA from biogenic VOCs by anthropogenic pollution could be an order-of-magnitude beyond what can be explained by current understanding. In a region like the Manaus metropolitan area, there are many anthropogenic sources, such as vehicular emissions, some products of industrial combustion, and electric power production. The deployment site is situated so that it experiences the extremes of a pristine atmosphere when the Manaus pollution plume meanders away and heavy pollution and the interactions of that pollution with the natural environment when the plume regularly intersects the site. The measurements at the deployment site will provide a unique dataset to address the interaction of biogenic and anthropogenic emissions.

New particle formation is another intended focus of IGRA2014. New particle formation is observed around the world in many forested environments. Yet over one year of measurements in pristine Amazon in the EUCAARI project showed the absence of new particle formation events, at least at ground level. New particles, however, must form somewhere in the Amazon Basin to sustain the existing particle concentration. Global chemical transport models suggest one part of the explanation: modeled H_2SO_4 concentrations are below the threshold of homogeneous nucleation. Therefore, a key measurement proposed for Amazonia is H_2SO_4 to test model accuracy. A recent study also suggests that large isoprene emissions can also suppress new particle formation in forests although the underlying mechanism for the suppression is unclear. (i) If modeled and measured H_2SO_4 concentrations are in agreement, then the question becomes, "What is the nucleation mechanism in the Amazon Basin?" Possibly it occurs in the upper troposphere. The answer to this question is important because in many aspects the atmospheric particle cycle of the Amazon Basin represents the world in 1750. If we delineate why this cycle is completely different in the Amazon Basin, then we can better quantify the perturbations to the atmospheric aerosol life cycle in regions affected by anthropogenic influence (e.g., northern boreal forest of Finland). (ii) If modeled and measured concentrations are in disagreement in that H_2SO_4 concentrations are high enough that new particle formation would be expected, the questions become, "Why are particle formation kinetics under the Amazon conditions different than elsewhere? If the suppression of new particle formation in the Amazon rainforest is due to high isoprene emission, what is the underlying mechanism?"

The concept of **cloud life cycle** encompasses a complex and interlocking set of physical processes. Cloud growth and cloud-scale organization are intimately connected with the initial thermodynamic state and convergent dynamical forcing, as well as the number and type of CCN. They are also linked tightly to surface fluxes of radiation, moisture, and heat. Individual clouds may merge into larger structures and these in turn may split into smaller cells, through a combination of internal circulation and regional-scale circulations. Cloud dissipation eventually occurs because of changes in forcing and adjustments in the larger-scale environment caused by fluxes of moisture, momentum, and possibly radiation that are in part cloud-driven. In the Amazon Basin, these factors generally interact to lead to scattered cumulus clouds in the lower troposphere between the surface and the freezing level[24] and strongly convective clouds that reach well into the upper troposphere and to the tropopause.[25] Data from the proposed deployment in the Basin will be used to explore the relationship of regional-scale dynamics to cloud life cycle, the influence of CCN microphysical properties and aerosol radiative heating profiles on cloud development and growth, the daily cycle of continental tropical convection (particularly the growth from shallow to deep convection), the role of landscape heterogeneity (such as the urban area of Manaus or km-scale rivers) on the dynamics of convection and clouds, and the evolution of convective intensity from severe storms in the dry season to moderate storms in the wet season.

The full three-dimensional spectrum of convective clouds from shallow, non-precipitating cumulus to deep, strongly precipitating cumulonimbus (including the associated anvil and cirrus clouds) will be one important focus for study. In support of this effort, a proposal is underway to request a deployment of the NCAR/EOL S-Pol. It is a dual wavelength (S- and K_a-band), polarized, Doppler radar. This scanning precipitation radar is a powerful tool for studying convective cloud processes and aerosol/land interactions. The dual-wavelength capability allows the retrieval of humidity and liquid water content profiles to better ascertain the environmental factors that influence the daytime shallow-to-deep convection transition. The polarimetric capability permits improved precipitation estimation and hydrometeor identification. Accurate rain maps are important for creating model forcing data sets and model evaluation. A dry bias in many present-day models of Amazonian rain fall might be leading to predictions of erroneous winds and sea surface temperatures in the Atlantic. Understanding this possible teleconnection is important for ascertaining susceptibility of regional climate to possible future changes. Rainfall is also a crucial component of diabatic heating, which is a main driver of the large-scale circulation in the tropics. Hydrometeor identification by S-Pol will also help to elucidate microphysical variations potentially due to aerosols and assist in assessing satellite retrievals. The Doppler capability enables full-volume observations of radial velocities in convective systems, thereby leading to a more quantitative understanding of the kinematics of storm evolution and organization and how these aspects vary spatially and with different aerosol concentrations. The envisioned deployment of S-Pol includes observations during the two planned IOPs in order to study wet and dry season convective storm dynamics in relation to the ground- and air-based measurements.

Another important aspect of IGRA2014 is a focus on the partitioning of the surface energy fluxes that affect cloud formation and that tend to occur more frequently in regions in which large sensible heat fluxes are coincident with a large latent heat fluxes, moisture convergence, or both. For example, fair-weather clouds are enhanced over deforested patches in the Amazon Basin where the sensible heat flux is greater.[26] Latent heat fluxes in this region are strongly modulated by evapotranspiration, which is controlled by water availability, plant physiology, leaf stomata, and atmospheric state variables including incoming solar radiation, temperature, and humidity. Hence, the advancing our understanding of the mechanics of evapotranspiration and its impacts upon the life cycle of shallow convection, which may transition to deep precipitating convection, is an important goal of IGRA2014, including the correct representation of these processes in models.

The radiation budget in the Amazon Basin is not yet fully constrained or quantified. Plant-atmosphere exchange processes and the partitioning of solar radiation into its direct and diffuse components provide the theoretical framework for land surface and atmosphere interactions. The partitioning of solar radiation is governed by cloud and aerosol properties that are entangled with photosynthesis-driven changes in the surface energy balance, boundary layer dynamics, and boundary layer moisture transports. The high atmospheric water vapor concentrations in the Amazon Basin lead to a special focus of IGRA2014 on the absorptive impact of this water vapor and the radiative effects of co-existing clouds. The net radiative heating rate of the atmospheric column above the Amazon Basin and its primary controls need to be measured, understood, and ultimately accurately modeled both at closure level and at GCM level.

With respect to **cloud-aerosol-precipitation interactions**, comparison among modeling results reveals that GCM simulations are highly sensitive to changes in cloud properties such as droplet concentration, droplet effective radius, the shape of the distribution, and liquid water content.[27-29]

Deep convective clouds play crucial roles in general circulation and the hydrological cycle. Many factors such as relative humidity and wind shear[30,6] have been proposed to explain the effects of aerosols on convection and precipitation. Over the Amazon, in-situ measurements indicate a suppression of low-level rainout and aerosol washout, which allows transport of water and smoke to upper levels, causing more intense thunderstorms.[4] For pristine conditions in the wet season, total particle concentrations average around 300 cm^{-3} in the Basin, which can be compared to contemporary background continental concentrations in the Northern Hemisphere of 2,000 to 3,000 cm^{-3}. These concentrations indicate a widespread anthropogenic influence on the Northern Hemisphere. Economic development in the Amazon Basin can therefore be anticipated to shift background particle concentrations to values much higher than 300 cm^{-3}. Cloud microphysical regimes are typically most sensitive to shifts of increasing CCN concentration from a few hundred up to 1000 cm^{-3}, above which there is often saturation with respect to the effects of increasing particle concentration. Within the Basin, both numerical simulations[9] and empirical studies[8] show that the sensitivity of precipitation to cloud microphysical properties is highly complex. Depending on environmental conditions, higher CCN concentrations can either increase or decrease total precipitation, as well as affecting the timing of precipitation in cloud systems. For instance, during the dry-to-wet season transition in the Amazon Basin, an increase in CCN concentration from biomass-burning aerosols leads to a decrease in the cloud droplet spectral dispersion, with direct consequences on the cloud reflectivity. Deployment of the G1 aircraft and, potentially, the S-Pol in the Amazon will provide new insights and an unprecedented dataset that can be used to improve cloud-aerosol-precipitation parameterizations for that region. More generally, the deployment in the Amazon Basin presents a unique opportunity for exploration of aerosol-cloud-precipitation interactions due to the expected wide range of aerosol concentrations and chemistry and the strong coupling between the vegetative surface, boundary layer, and convective initiation. This knowledge can be critically important for understanding of tropical precipitation.

Analysis **integrating the carbon cycle, the aerosol life cycle, the cloud life cycle, and aerosol-cloud interactions** will make use of observations and models of different scales. Box or one-dimensional models are most appropriate for detailed analysis of the time development of the Manaus plume. Large-eddy simulations and cloud-resolving modeling simulations are the main theoretical tools to link aerosol and cloud microphysical measurements, conduct process studies to understand the mechanisms of aerosol indirect effects, and look into aerosol-cloud-precipitation interactions under different atmospheric conditions. Size-resolved cloud microphysics can be employed to understand how different types and size distribution of aerosols change cloud processes, and thereby affect cloud cover, cloud lifetime, and radiative forcing.

The proposed IGRA2014 project under the umbrella of GoAmazon2014 leverages into many past, existing, and planned activities in the Amazon Basin, including but not limited to the Large-Scale Biosphere-Atmosphere Experiment in Amazonia (LBA), GPM-CHUVA, Aeroclima, ATTO, BEACHON, IARA2014, AMF2014, SPOL, NASAsatellites, iLEAPS→IGAC→ACPC, the T2→T3 Quasi-Lagrangian Experiment, SAMBBA, Amazon-PIRE, and the Andes-Amazon Initiative.

As one example, the CHUVA experiment, meaning Cloud processes of tHe main precipitation systems in Brazil: A contribUtion to cloud resolVing modeling and to the GPM (GlobAl Precipitation Measurement; http://chuvaproject.cptec.inpe.br/portal/en/index.html), will be closely coordinated with the wet season IOP of IGRA2014. Near K34 or EMBRAPA, CHUVA

will bring the following equipment: Field Mill, GPS, microwave radiometer (MP3000), Joss and Parsivel disdrometer, raingauge, micro rain radar (MRR), soil moisture, heat, moisture, and CO_2 flux. Within 20 km, there will be three more sites equipped with raingauges, disdrometers, and GPS, with a high likelihood of another another MRR and field mill at at least one of these sites. There will also be three radiosonde stations (4 sondes/day) for 10 days of the IOP in a triangle in T1, T3, and K34. In addition, for the duration of the IOP, there will one radiosonde site, having one balloon/day. A Brazilian proposal is under way to retain an X-Pol radar during this IOP. If this proposal is successful, the radar will be installed to provide coverage of K34 and T3, ideally at location between the two sites. An additional possibility for IGRA2014 will be balloon flights that follow up on successful tests of a new instrument in CHUVA Belem in June 2011 (http://www.science.smith.edu/cmet/flight.html). An updated version with a CO_2 sensor is under development, and a possibility for IGRA2014 could be to launch 3 balloons at the same time but different heights to compute CO_2 convergence/divergence in a quasi lagrangian atmosphere boundary layer observation, toward the goal of improving the understanding of the diel variability of CO_2.

In summary, the proposed research responds to the societal need to have a prognostic capability of the changes in terrestrial ecosystems, clouds, radiative balance, climate, and feedbacks among them in response to perturbations of the inputs into the natural tropical systems by urbanization. Implicit in these objectives is an intellectual focus on understanding and quantifying the differences between pristine and anthropogenically influenced air masses in the tropical environment. The purpose is that the development of this knowledge base concerning the influences of anthropogenic activities in a tropical environment can be combined with past and projected demographic changes to determine, through model simulation, how encroachment of urban areas on forests has in the past and will in the future affect radiative forcing, aspects of the hydrologic cycle, and the evolution of regional and global climate.

Education and Training

This segment is very important in the context of IARA2014 as the data collection and the physical/chemical characterization of the atmosphere is not well known by the Brazilian scientific community. The AAF will conduct two field missions during IARA 2014 of 40 days each (one will be during March-April for the wet season and the second one will be Sept-Oct in order to characterize the dry season). For each of them, the experiment will involve scientists and students for the data-collection. The post-processing of data will be conducted by Brazilians, after training by their International counterparts.

We also envisage enrolling Universities and Research Centers into this segment. Locally, the major organizations are UEA, INPA, FUA, SIPAM, and EMBRAPA. They will be contacted, involved in the process, and requested to provide personnel (scientists and students). Moreover, others Universities and Research Centers that are traditionally involved in the Amazon studies within LBA will be contacted. For example, in Belem, several organizations are fully involved in LBA's activities (e.g., UFPA-Meteorology Faculty, UFRA -Meteorology group, EMBRAPA). From other parts of Brazil, there are also several organizations studying the Amazon (e.g., UFSM, USP, CTA/IAE, INPE, UFAL, UFV, among others) that will be involved as well.

In addition to the work conducted during the field campaign, it is desirable to have in Manaus a field course (1 full week with theoretical and practical, hands-on training) where Scientists will

give a complete description of the instruments deployed (both for the surface ARM and aerial AAF components). This course will be organized by the local participants (INPA and/or UEA) and it is projected to have 20-25 students (MSc and PhD levels). It can be associated as a special course to the Climate and Environments (MSc and PhD) Programs at INPA/UEA in Manaus.

For the data analysis phase, an interchange of students (mainly PhD students) among the senior participants from Brazil and foreigner counterparts will be established, identifying mutual interests and potential collaborations. From the Brazilian side, the "sandwich scheme" (usually promoted by CAPES and CNPq) can be used. Recently, the Federal Government of Brazil, through the Science and Technology Minister (MCT) has launched a new program ("Ciência Sem Fronteiras - Science without Frontiers) that can distribute and sponsor scholarships for short duration courses (up to 1 academic year) outside of Brazil. The US and others countries have a list of potential Universities that can receive these students (from different levels of education – MSc and/or PhD students). Other sponsoring Agencies (like FAPEAM, FAPESP, CNPq, CAPES, Fulbright Foundation, etc) will be contacted.

Finally, it should be emphasized that the greatest legacy of this experiment for the Amazonian (and Brazilian) community is the expertise (both knowledge and training/education) that will be transferred through the joint work between Brazilian and Foreign Scientists and Students.

References Cited

(1) Zhou, J. Y.; Lau, K. M. "Does a monsoon climate exist over South America?," *Journal of Climate*, **1998**, *11*, 1020.

(2) Wang, H.; Fu, R. "The influence of Amazon rainfall on the Atlantic ITCZ through convectively coupled Kelvin waves," *Journal of Climate*, **2007**, *20*, 1188.

(3) Williams, E.; Rosenfeld, D.; Madden, N.; Gerlach, J.; Gears, N.; Atkinson, L.; Dunnemann, N.; Frostrom, G.; Antonio, M.; Biazon, B.; Camargo, R.; Franca, H.; Gomes, A.; Lima, M.; Machado, R.; Manhaes, S.; Nachtigall, L.; Piva, H.; Quintiliano, W.; Machado, L.; Artaxo, P.; Roberts, G.; Renno, N.; Blakeslee, R.; Bailey, J.; Boccippio, D.; Betts, A.; Wolff, D.; Roy, B.; Halverson, J.; Rickenbach, T.; Fuentes, J.; Avelino, E. "Contrasting convective regimes over the Amazon: Implications for cloud electrification," *Journal of Geophysical Research-Atmospheres*, **2002**, *107*, 8082.

(4) Andreae, M. O.; Rosenfeld, D.; Artaxo, P.; Costa, A. A.; Frank, G. P.; Longo, K. M.; Silva-Dias, M. A. F. "Smoking rain clouds over the Amazon," *Science*, **2004**, *303*, 1337.

(5) Rosenfeld, D.; Lohmann, U.; Raga, G. B.; O'Dowd, C. D.; Kulmala, M.; Fuzzi, S.; Reissell, A.; Andreae, M. O. "Flood or drought: How do aerosols affect precipitation?," *Science*, **2008**, *321*, 1309.

(6) Khain, A.; Lynn, B. "Simulation of a supercell storm in clean and dirty atmosphere using weather research and forecast model with spectral bin microphysics," *Journal of Geophysical Research-Atmospheres*, **2009**, *114*, D19209.

(7) Laurance, W. F.; Williamson, G. B. "Positive feedbacks among forest fragmentation, drought, and climate change in the Amazon," *Conservation Biology*, **2001**, *15*, 1529.

(8) Lin, J. C.; Matsui, T.; Pielke, R. A.; Kummerow, C. "Effects of biomass-burning-derived aerosols on precipitation and clouds in the Amazon Basin: a satellite-based empirical study," *Journal of Geophysical Research-Atmospheres*, **2006**, *111*, D19204.

(9) Martins, J. A.; Dias, M.; Goncalves, F. L. T. "Impact of biomass burning aerosols on precipitation in the Amazon: A modeling case study," *Journal of Geophysical Research-Atmospheres*, **2009**, *114*, D02207.

(10) Andreae, M. O. "Aerosols before pollution," *Science*, **2007**, *315*, 50.

(11) Cox, P. M.; Betts, R. A.; Collins, M.; Harris, P. P.; Huntingford, C.; Jones, C. D. "Amazonian forest dieback under climate-carbon cycle projections for the 21st century," *Theoretical and Applied Climatology*, **2004**, *78*, 137.

(12) McDowell, N. G.; Sevanto, S. "The mechanisms of carbon starvation: how, when, or does it even occur at all?," *New Phytologist*, **2010**, *186*, 264.

(13) Farquhar, G. D.; Roderick, M. L. "Pinatubo, diffuse light, and the carbon cycle," *Science*, **2003**, *299*, 1997.

(14) Doughty, C. E.; Flanner, M. G.; Goulden, M. L. "Effect of smoke on subcanopy shaded light, canopy temperature, and carbon dioxide uptake in an Amazon rainforest," *Global Biogeochemical Cycles*, **2010**, *24*, 3015.

(15) Kuhn, U.; Ganzeveld, L.; Thielmann, A.; Dindorf, T.; Welling, M.; Sciare, J.; Roberts, G.; Meixner, F. X.; Kesselmeier, J.; Lelieveld, J.; Ciccioli, P.; Kolle, O.; Lloyd, J.; Trentmann, J.; Artaxo, P.; Andreae, M. O. "Impact of Manaus City on the Amazon Green Ocean atmosphere: Ozone production, precursor sensitivity and aerosol load," *Atmospheric Chemistry and Physics*, **2010**, *10*, 9251.

(16) Artaxo, P.; Martins, J. V.; Yamasoe, M. A.; Procopio, A. S.; Pauliquevis, T. M.; Andreae, M. O.; Guyon, P.; Gatti, L. V.; Leal, A. M. C. "Physical and chemical properties of aerosols

in the wet and dry seasons in Rondonia, Amazonia," *Journal of Geophysical Research-Atmospheres*, **2002**, *107*, 8081.
(17) Machado, L. A. T.; Laurent, H.; Dessay, N.; Miranda, I. "Seasonal and diurnal variability of convection over the Amazonia: A comparison of different vegetation types and large scale forcing," *Theor. Appl. Climatol.*, **2004**, *78*, 61.
(18) Hall, S. J.; Matson, P. A. "Nitrogen oxide emissions after nitrogen additions in tropical forests," *Nature*, **1999**, *400*, 152.
(19) Mo, J. M.; Zhang, W.; Yu, G. R.; Fang, Y. T.; Li, D. J.; Lu, X. K.; Wang, H. "Emissions of nitrous oxide from three tropical forests in Southern China in response to simulated nitrogen deposition," *Plant and Soil*, **2008**, *306*, 221.
(20) Reay, D. S.; Dentener, F.; Smith, P.; Grace, J.; Feely, R. A. "Global nitrogen deposition and carbon sinks," *Nature Geoscience*, **2008**, *1*, 430.
(21) Wang, H. L.; Zhang, X.; Chen, Z. M. "Development of DNPH/HPLC method for the measurement of carbonyl compounds in the aqueous phase: applications to laboratory simulation and field measurement," *Environmental Chemistry*, **2009**, *6*, 389.
(22) Shilling, J. E.; Chen, Q.; King, S. M.; Rosenoern, T.; Kroll, J. H.; Worsnop, D. R.; DeCarlo, P. F.; Aiken, A. C.; Sueper, D.; Jimenez, J. L.; Martin, S. T. "Loading-dependent elemental composition of alpha-pinene SOA particles," *Atmospheric Chemistry and Physics*, **2009**, *9*, 771.
(23) Aiken, A. C.; Decarlo, P. F.; Kroll, J. H.; Worsnop, D. R.; Huffman, J. A.; Docherty, K. S.; Ulbrich, I. M.; Mohr, C.; Kimmel, J. R.; Sueper, D.; Sun, Y.; Zhang, Q.; Trimborn, A.; Northway, M.; Ziemann, P. J.; Canagaratna, M. R.; Onasch, T. B.; Alfarra, M. R.; Prevot, A. S. H.; Dommen, J.; Duplissy, J.; Metzger, A.; Baltensperger, U.; Jimenez, J. L. "O/C and OM/OC ratios of primary, secondary, and ambient organic aerosols with high-resolution time-of-flight aerosol mass spectrometry," *Environmental Science and Technology*, **2008**, *42*, 4478.
(24) Koren, I.; Kaufman, Y. J.; Remer, L. A.; Martins, J. V. "Measurement of the effect of Amazon smoke on inhibition of cloud formation," *Science*, **2004**, *303*, 1342.
(25) Hartmann, D. L. *Global Physical Climatology*; Academic Press: San Diego, 1994.
(26) Chagnon, F. J. F.; Bras, R. L.; Wang, J. "Climatic shift of patterns of shallow cumulus over the Amazon," *Geophys. Res. Lett*, **2004**, *31*, L24212.
(27) Dandin, P.; Pontikis, C.; Hicks, E. "Sensitivity of a GCM to changes in the droplet effective radius parameterization," *Geophysical Research Letters*, **1997**, *24*, 437.
(28) Liu, Y. G.; Daum, P. H. "Anthropogenica erosols - Indirect warming effect from dispersion forcing," *Nature*, **2002**, *419*, 580.
(29) Rotstayn, L. D.; Liu, Y. G. "Sensitivity of the first indirect aerosol effect to an increase of cloud droplet spectral dispersion with droplet number concentration," *Journal of Climate*, **2003**, *16*, 3476.
(30) Fan, J. W.; Yuan, T. L.; Comstock, J. M.; Ghan, S.; Khain, A.; Leung, L. R.; Li, Z. Q.; Martins, V. J.; Ovchinnikov, M. "Dominant role by vertical wind shear in regulating aerosol effects on deep convective clouds," *Journal of Geophysical Research-Atmospheres*, **2009**, *114*, D22206.

ANEXO 12

6th GLM-CHUVA Planning Meeting

MINUTE

08 August 2011, 5:30pm @ Room Vidigal B/C

1) List of CHUVA instrumentation and satellite imagery (Albrecht, Machado, Morales)

List of instrumentation distributed.

Area of coverage? 500 km radius around LMA center

2) Network status (shipping and deployment schedule)

- LMA (Blakeslee), (online LMA map)

  11 sites are identified and 3 are remaining to be surveyed: Seminário São Tomás de Aquino, Arujá e Mogi das Cruzes. 2 of the west sites (UAB and Mackenzie), will be substituted by Arujá and Mogi das Cruzes if these sites are as good as the previous ones at west. Baseline: ~15km

- LINET (Holler), (online LINET map)

  Instruments are at USP and will be deployed in 2 weeks or so. Baseline: ~30km.

- TLS200 (Lojou), (online TLS200 map)

  3 sites were identified and 2 are remaining: Juquitiba and PUC. They will be surveyed next week. Baseline: ~100km.

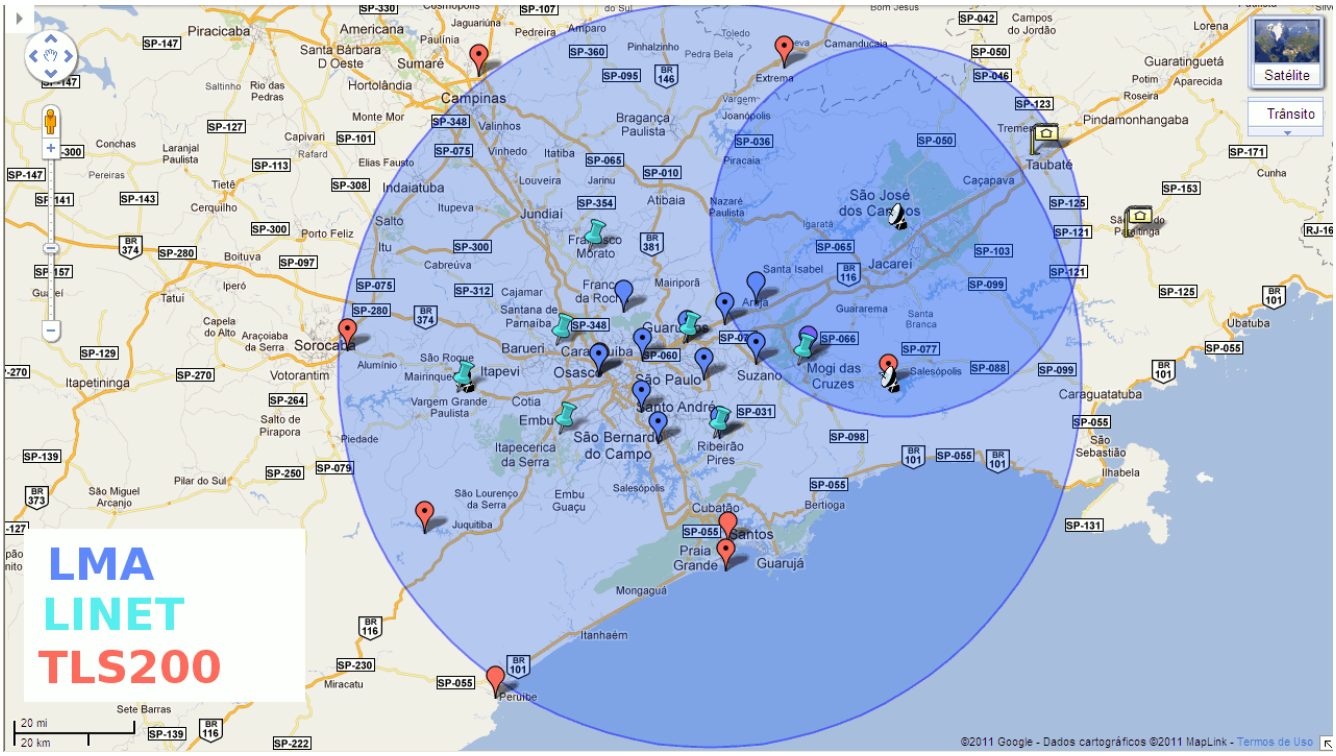

- Weatherbug (Pinto, Naccarato, Anderson, Heckman)

19 stations are operating in São Paulo, Minas Gerais and Bahia, with ~250km baselines

More sensors will be deployed in a shorter baseline. Number of sensor and baseline are to be defined.

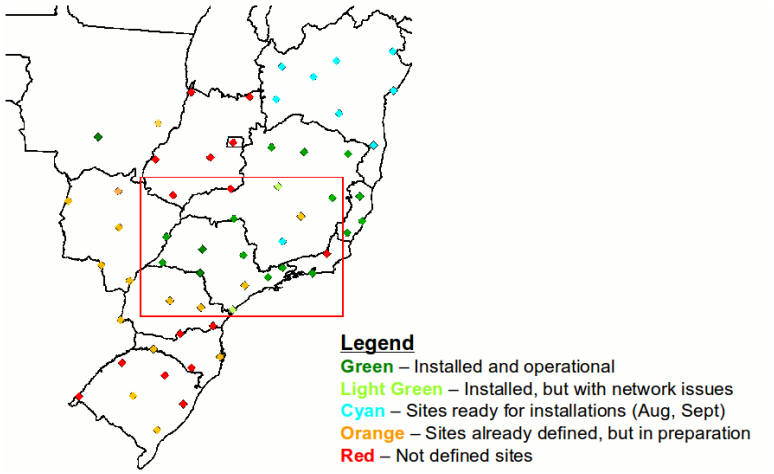

3) Legal issue: REAL TIME DATA IS MANDATORY (Albrecht)

Clarifying Clause 11 of the MOU to better suite Brazil's Ministry of Science and Technology rules: A copy of all data collected in Brazil have to stay in Brazil, so **it is *mandatory* that the real time (or near real time) be sent to CHUVA archive.**

4) CHUVA Data Archive. (Albrecht, Goodman)

A) Data nomenclature:

Level 0: Raw data (waveforms) → **not** available to the archive
Level 1a: Real time solutions
Level 1b: Reprocessed quality assured solutions
Level 2: CG, IC

B) What and how to provide data to the archive:

- Levels 1a, 1b and 2 (if applicable).

- Via FTP to "pararaca.cptec.inpe.br" (150.163.133.228)
  We will create an account for each instrument.
  For example:
  username: lma
  password: lma1234

  Directory structure:
  LMA
  LINET
  TLS200
  LS7001
  RINDAT
  WTLN
  High_speed_camera
  Delta_E
  etc...

- All other CHUVA data (radar, rain gauges, disdrometers, etc. - non-lightning related) can be accessed via FTP at:
  possanga.cptec.inpe.br
  username: chuvaproject
  password: chuvAgpm

- In the future a web-based home page will made available with a friendly access and data search.

C) Who has access to real time data (Level 1a)?

CHUVA-GLM only. Regular CHUVA participants will not have access to Level 1a, only Level 1b and beyond. However, images of real time data will be publicly available at the website.
Level 1a data cannot be used for instrument intercomparison without consent of the data provider.

D) Time frame for Level 1b and 2 data to be available at CHUVA archive.

1 month after they are collected for the lightning location systems, field mills and delta-E antennas. Video related data will be available as they become time tagged, etc..

E) Each data provider will provide reports of the status of their Level 1b and Level 2 datasets.

No need for reports due to the requirement of data availability in 1 month after they are collected.
However, a metadata and data summary is required. Also a one-two paragraphs about your instrumentation description is required.

F) Data format:

ASCII with latitude, longitude, (and altitude, polarity, multiplicity and classification (IC,CG) when applied) of sources, strokes, flashes, etc.
If the data is not in ASCII the data provider need to provide documentation and a script to convert the data into ASCII.

G) Area of coverage:

Any solution within 500 km radius of LMA center. LMA center coordinates will be provided after the deployment of the system.

5) Nowcasting and alert systems (Machado, Morales)

- A *public* website will be designed to disseminate the available data and products for public use (emergency managers). In this sense, Level 1a data from all networks will be displayed *as images*, at this website, combined or not with other data.
- The website will also host lightning nowcasting/alert products developed by the data providers if permitted they are interested. CHUVA scientists will develop their own algorithms and nowcasting/alert products using the real time data generated by the networks. If you are interested please contact Rachel Albrecht (rachel.albrecht@cptec.inpe.br).

6) Extension of radar operation / campaign. (Machado, Morales)

- We are gathering funds to extend the operations of X-POL radar (total cost: USD 15K/month). If you are interested in collaborate, please contact Rachel Albrecht, Carlos Morales or Steve Goodman.
- Up to which date could the networks stay?
  CHUVA instrumentation (up to March)
  LMA (end of June/July), LINET (end of March), TLS200 (end of March)
  Remaining "fixed" networks data available during the extended period? Yes.
  Field Mills, cameras? Yes.

7) IOP daily discussions (Machado)

During the IOP (1 Nov to 23 Dec 2011) we will have daily discussions at CHUVA headquarters. Daily weather briefing and measurement review of the day before.
We will provide a Skype/Webex type for those who want to participate remotely.

8) Data intercomparison (Goodman)

A) After Level 1b and Level 2 data is released:

- How will the network inter-comparisons be conducted?
  Suggestion: **Collaborative** effort: as we don't know the ins and outs of other system providers.
  Each data provider provides details on the measurements they took and then we should work together on specific intercomparisons.

B) Create a committee with one person representing each party. For example:
"GOES-R and GLM": Steve Goodman
CHUVA: Rachel Albrecht and Luiz Machado
LMA: Richard Blakeslee
LINET: Hartmut Holler
TLS200: Vaisala TBD
STARNET: Carlos Morales
BrasilDAT(RINDAT+Weatherbug): Osmar Pinto, Kleber Naccarato and Stan Heckman
WWLLN: Robert Holzworth
GLD360: Vaisala TBD
ATDnet: Alec Bennett
WSI: Kim Rauenzahn, Carlos Morales and Osmar Pinto
Field Mills: Marcos Ferro
Cameras: Marcelo Saba and Antonio Saraiva
TLE: Fernada São Sabbas

C) An official report on the data inter-comparison will be released trough a WMO document.
Who will lead? Volunteers? (Rachel Albrecht,Steve Goodman (as collaborator), Carlos Morales, ….....)
(*everyone* involved will be a co-author!!!)

9) Public Outreach and press releases (Goodman)

Iara Cardoso- Osmar's daughter is a TV producer and agreed earlier to visit sites and take video and help put together a package we can all use for our press releases. I asked if she was attending the meeting. She could for example begin interviewing the principals at the ICAE, later visit sites, take some video at the experiment control center, etc.

10) CHUVA Science Team Workshop- date?

May 2012 (?).

ANEXO 13

CHUVA INSTRUMENTATION FOR SÃO LUIZ DO PARAITINGA IOP (rain-atmosphere related instruments)

Instrument	Site name
X-band Dual Polarimetric radar	UNIVAP, São José dos Campos
Radiosonde	CPTEC, Cachoeira Paulista
Radiosonde	Ubatuba
Radiosonde	CTA, São José dos Campos
Vertical pointing radar	UNITAU, Taubaté
Vertical pointing radar	Núcleo Santa Virginia, São Luiz do Paraitinga
Vertical pointing radar	To be determined
Rain gauge NASA	UNITAU, Taubaté
Rain gauge NASA	UNIVAP, São José dos Campos
Rain gauge NASA	Núcleo Santa Virginia, São Luiz do Paraitinga
Rain gauge NASA	UNITAU, Taubaté
Rain gauge NASA	Núcleo Santa Virginia, São Luiz do Paraitinga
Rain gauge INPE	Usina Cel. Abner
Rain gauge INPE	Usina Cel. Abner
Rain gauge INPE	CTA, São José dos Campos
Rain gauge INPE	CTA, São José dos Campos
Rain gauge INPE	CPTEC, Cachoeira Paulista
Disdrometer Joss-Wadvogel	UNITAU, Taubaté
Disdrometer Parsivel	UNITAU, Taubaté
Disdrometer Parsivel	Núcleo Santa Virginia, São Luiz do Paraitinga
Disdrometer Parsivel	Usina Cel. Abner
GPS	UNITAU, Taubaté
GPS	Núcleo Santa Virginia, São Luiz do Paraitinga
Microwave Profiling Radiometer	UNITAU, Taubaté
Lidar	UNITAU, Taubaté
Flux tower	UNITAU, Taubaté
Soil humidity	UNITAU, Taubaté
Meteorological Surface Station	UNITAU, Taubaté

CHUVA INSTRUMENTATION FOR SÃO LUIZ DO PARAITINGA IOP
(lightning related instruments)

Instrument	Site name
Lightning Mapping Array	USP Pelletron, São Paulo
Lightning Mapping Array	USP Leste, São Paulo
Lightning Mapping Array	Morro da Igreja, Ribeirão Pires
Lightning Mapping Array	Parque CienTec, São Paulo
Lightning Mapping Array	Parque do Carmo, São Paulo
Lightning Mapping Array	CEFET, Suzano
Lightning Mapping Array	UNIFESP, Guarulhos
Lightning Mapping Array	CEFET, São Paulo
Lightning Mapping Array	FEI São Bernardo do Campo
Lightning Mapping Array	Seminário São Tomás de Aquino, Caieiras
Lightning Mapping Array	TBD, Arujá
Lightning Mapping Array	TBD, Mogi das Cruzes
LINET	Universidade Mackenzie, Barueri
LINET	USP Leste, São Paulo
LINET	Radar DECEA, São Roque
LINET	Univesidade Aberta do Brasil, Itapecirica da Serra
LINET	Morro da Igreja, Ribeirão Pires
LINET	TBD, Mogi das Cruzes
LINET	TBD, Francisco Morato
TLS200	UNISO, Sorocaba
TLS200	PUC, Campinas
TLS200	Morro da Oi, Extrema
TLS200	Barragem Ponte Nova, Salesópolis
TLS200	Forte Duque de Caxias, Praia Grande
TLS200	Represa Cachoeira do Fraça, Juquitiba
High speed camera (??? fps)	Torre CTA, São José dos Campos
High speed camera (??? fps)	CTA, São José dos Campos
High speed camera (??? fps)	Av. Paulista, São Paulo
"Fast" electric field sensor (306Hz-1.5MHz)	Torre CTA, São José dos Campos
"Slow" electric field sensor (1Hz-300MHz)	Torre CTA, São José dos Campos
Field Mill – CTA/IAE	Banco de provas de 1000 kN da UCA
Field Mill – CTA/IAE	Torre CTA, São José dos Campos
Field Mill – CTA/IAE	Prédio da Administração da CCR Nova Dutra em Santa Isabel
Field Mill – CTA/IAE	Cabine Primária da Praça de Pedágio em Jacareí
Field Mill – CTA/IAE	Prédio do CESAP da Prefeitura Municipal de Guararema
Field Mill – CTA/IAE	Prédio do PSF da Prefeitura Municipal de Igaratá
Field Mill – FEI	FEI São Bernardo do Campo
Field Mill – USP (Boltek)	To be determined
Field Mill – USP (Boltek)	To be determined
Field Mill – USP ("FieldMilk")	To be determined
Field Mill – USP ("FieldMilk")	To be determined
Field Mill – USP ("FieldMilk")	To be determined
Field Mill – USP ("FieldMilk")	To be determined
Field Mill – CHUVA	UNITAU, Taubaté
Field Mill – CHUVA	Núcleo Santa Virginea, São Luiz do Paraitinga
RINDAT	Brazil
STARNET	Brazil
WWLLN	Brazil

ANEXO 14

THE SÃO PAULO LIGHTNING MAPPING ARRAY (SPLMA): PROSPECTS FOR GOES-R GLM AND CHUVA

Rachel I. Albrecht[1,2]*, Richard J. Blakeslee[3], Jeffrey C. Bailey[4], Larry Carey[4], Steven J. Goodman[5,6], Eric C. Bruning[2], William Koshak[4], Carlos A. Morales[7], Luiz A. T. Machado[1], Carlos F. Angelis[1], Osmar Pinto Jr.[8], Kleber Naccarato[8], Marcelo Saba[8]

[1]Instituto Nacional de Pesquisas Espaciais, Cachoeira Paulista, SP, Brazil
[2]Cooperative Institute for Climate and Satellites – UMD/NOAA, College Park, MD, USA
[3]Marshal Space Flight Center – NASA, Huntsville, AL, USA
[4]University of Alabama-Huntsville, Huntsville, AL, USA
[5]National Environmental Satellite, Data, and Information – NOAA, Camp Springs, MD
[6]Goddard Space Flight Center – NASA, Greenbelt, MD, USA
[7]Universidade de São Paulo, São Paulo, SP, Brazil
[8]Instituto Nacional de Pesquisas Espaciais, São José dos Campos, SP, Brazil

***rachel.albrecht@cptec.inpe.br**

RESUMO: Este trabalho apresenta as características e as perspectivas de um "*Lightning Mapping Array*" a ser implantado na cidade de São Paulo (SPLMA). Esta rede LMA irá fornecer à campanha CHUVA raios totais, mapeamento do canal de raios e informações detalhadas sobre os locais responsáveis pelas regiões de cargas das nuvens de tempestade investigadas durante um de seus períodos de observação intensiva. A disponibilidade em tempo real das observações do LMA também irá contribuir para a concientização da situação meteorológica e apoio à execução da missão do CHUVA. Para o programa do GOES-R irá formar uma base de dados "proxy" única e valiosa para ambos os sensores GLM e ABI em apoio à vários questões de pesquisa em curso.

ABSTRACT: This paper presents the characteristics and prospects of a Lightning Mapping Array to be deployed in São Paulo (SPLMA). This LMA network will provide the CHUVA campaign with total lightning, lightning channel mapping and detailed information on the locations of cloud charge regions for the thunderstorms investigated during one of its Intensive Observation Periods (IOP). The real-time availability of LMA observations will also contribute to and support improved weather situational awareness and mission execution. For the GOES-R program it will form the basis of generating unique and valuable proxy data sets for both the GLM and ABI sensors in support of several on-going research investigations.

Palavras-chave: raios, relâmpagos, sistemas de localização de raios, CHUVA, GLM.

1 – INTRODUCTION

Lightning flashes have been the object of interest and research for decades. Thunderstorm lightning activity is tightly controlled by the updraft intensity and ice precipitation formation in the clouds, which makes it closely related to storm dynamics and microphysics. Therefore, cloud electrification conveys useful information about the rate, amount and distribution of convective precipitation (Goodman and Buechler, 1990; Petersen 1998; Cecil et al., 2005; Liu et al., 2008), as well as severe weather (Williams et al., 1999, Schultz et al., 2009, Gatlin and Goodman, 2010) with potential threats to life, wild fires and damages to structures and facilities. All these implications make the location of lightning occurrence of high interest to several sectors of society. In this matter, lightning location systems (LLS) have been in operation over many decades.

LLS are based on the detection of the electromagnetic radiation emitted by lightning, which can be done mainly using radio and optical frequencies. Radio emissions from lightning occur in the form of short pulses by accelerated charges during the fast changing current steps, while the optical emissions occur from ionized and dissociated gases by thermal radiation of the lightning channel (Christian and Goodman, 1987). High energetic processes of lightning (e.g., return strokes) can be detected on the range of low (LF) to very low (VLF) radio frequencies (Cummins and Murphy 2009). Other processes (e.g., less energetic breakdown processes) are only detected by very high frequencies (VHF). Most of the LLS operational worldwide are networks of LF and VLF sensors, which makes possible the location of lightning (mainly cloud-to-ground, CG) occurrence in space and time only in two-dimensional coordinates (i.e., latitude and longitude).

The New Mexico Institute of Mining and Technology developed a detection system called the Lightning Mapping Array (LMA) (Rison et al. 1999), based on the Lightning Detecting and Ranging (LDAR) system developed to be used at the NASA Kennedy Space Center (Maier et al. 1995). The LMA system locates the peak source of impulsive VHF radio signals from lightning in an unused television channel by measuring the time-of-arrival of the magnetic peak signals at different receiving stations in successive 80 μ s intervals. Hundreds of sources per flash can be detected in space and time, allowing a three-dimensional (3-D) lightning map to be constructed with nominally <50 m error within 150 km (Goodman et al. 2005). Figure 1a illustrates the time-of-arrival approach used in the LMA system. Global Positioning System (GPS) receivers at each station provide both accurate signal timing and station location knowledge required to apply this approach. Figure 1b is a picture of a portable LMA station hardware.

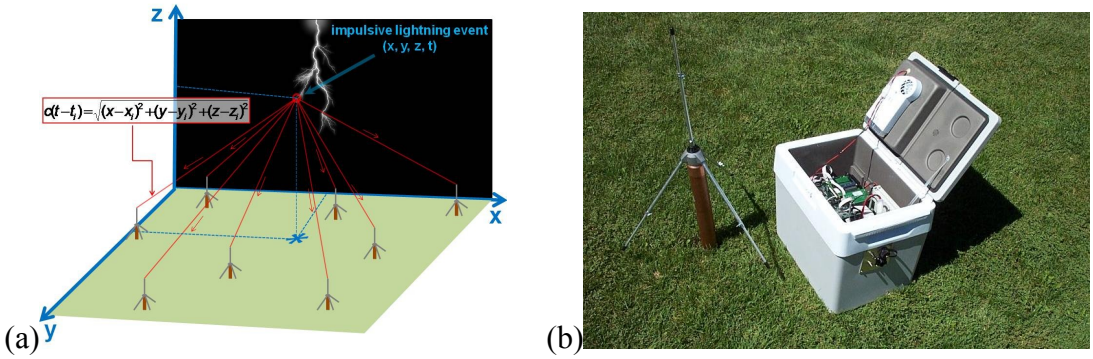

(a) (b)

Figure 1 – (a) Illustration of the time-of-arrival technique used by the LMA system. The times (t_i) when a signal is detected at N≥4 stations are used to solve for the 3D source location ($\underline{x}$, y, z, t) of the impulsive breakdown processes associated with a discharge. (b) Portable LMA station electronic box and antenna.

In the United States there are research and operational VHF lightning mapping systems (LMAs in New Mexico, Oklahoma (OKLMA), Alabama (NALMA) and Washington D.C. (DCLMA), and LDARs in Houston, Texas and Kennedy Space Center, Florida). These networks provide 3-D total lightning (i.e. cloud-to-ground and intracloud) data for local weather service offices and national prediction centers, where it is used in the severe weather forecast and warning decision-making process. Total lightning information gives us a complete picture of the thunderstorm electrification and lightning activity, which is not possible using conventional LF and VLF networks where mostly only CG lightning is detected, although VHF networks not providing precise information of CG lightning ground contacts should be complemented by LF and VLF networks.

LMA data is being used as proxy data for the upcoming Geostationary Lightning Mapper (GLM) optical sensor onboard the GOES-R satellite. GOES-R is scheduled to be launched in late 2015 and will also carry the Advanced Baseline Imager (ABI). ABI is a visible and infrared imager that offers significant improvements over the current generation of

GOES imager in spectral-band coverage, spatial resolution, and sampling frequency. The GLM was built on the heritage of the NASA Optical Transient Detector (OTD) and the Lightning Imaging Sensor (LIS), consistent of a wide field-of-view telescope focused on a high speed charge coupled device (CCD), combined with a narrow band interference filter centered on 777.4 nm (Christian et al, 2000; Christian et al., 2003). The signal is read out from the focal plane into a real-time event processor for event detection, which are sent to the satellite ground station for geolocation processing in space and time, resulting in a "flash" (multiple CCD events grouped into time and space).

The GOES-R Algorithm Working Group (AWG) is developing and validating operational algorithms that will use products from GOES-R instruments so that these algorithms will be ready for use on "day 1" following GOES-R launch. During this pre-launch phase, these activities rely on the generation and use of proxy and simulated instrument data sets to develop, validate and test products and data processing. LMA total lightning from the United States networks are being used to generate the necessary GLM proxy data. In addition, the ABI proxy data can be derived from SEVERI (Spinning Enhanced Visible and Infrared Imager) onboard of the Meteosat Second Generation (MSG) satellite, which does not cover the United States. Therefore, a unique opportunity to acquire collocated ABI and GLM proxy data, as well as intensive atmospheric measurements to validate and calibrate GOES-R candidate algorithms, will be the CHUVA ("***C***loud processes of t***H***e main precipitation systems in Brazil: A contrib***U***tion to cloud resol***V***ing modeling and to the GPM (Glob***A***l Precipitation Measurement)") field campaign. CHUVA project covers climate and physical processes studies using conventional and special observations (polarimetric radar, radiometer, LIDAR, etc) to create a database describing the cloud processes of the main precipitating system in Brazil. It intends to create and exploit this database to improve remote sensing precipitation estimation, rainfall ground validation and microphysical parameterizations of the tri-dimensional characteristics of the precipitating clouds.

Thereby, the deployment of a LMA network to Brazil will occur during one of CHUVA's Intensive Observation Periods (IOP). This effort will acquire unique total lightning proxy data from the LMA to the GLM collocated to SEVRI proxy data for ABI. The next session describes the proposed network.

2 – THE SAO PAULO LIGHTNING MAPPING ARRAY (SPLMA)

The first CHUVA IOP was conducted in Alcantara, Ceara state, in March and April of 2010. The objective of this first IOP was to study warm clouds, tropical squall lines and easterly waves. The second IOP will be conducted in São Luiz do Paraitinga, São Paulo state, Brazil, from December 2010 to January 2011, in order to learn more about the South Atlantic Convergence Zone (SACZ), local convection and enhancement of orographic precipitation. São Luiz do Paraitinga is near one of the biggest cities in the world, São Paulo (about 150 km). São Paulo has a unique infrastructure in the Latin America which makes the perfect place to deploy a LMA network. Moreover, as a mega urban center, the city constantly suffers with flash floodings and severe weather, where the potential nowcasting algorithms based on LMA measurements could be developed and tested with a very high value to the society.

The total lightning activity over the city of São Paulo and São Luiz do Paraitinga are shown in Figure 2. Moderate (10-30 fl km^{-2} yr^{-1}) to high (>30 fl km^{-2} yr^{-1}) lightning activity is observed along São Paulo state coast (Figure 2a). São Paulo's east coast is composed of two sets of high elevated terrain (> 1500 m) with a valley (Paraiba Valley) in between, where São Luiz do Paraitinga is located. The annual cycle of lightning over these regions (Figure 2b) show a minimum (<5 fl day^{-1}) from June to August (austral winter) and a gradually increase from September (~15 fl day^{-1}) to November (~42 fl day^{-1}). A steep increase during the summer is observed: ~40 fl day^{-1} in December jumps to a peak in February of 57 fl day^{-1} for

São Luiz do Paraitinga and 71 fl day^{-1} for São Paulo. The reason for a higher peak in the city of São Paulo is believed to be related to the enhancement of deep convection by the urban heat island, which will also be studied during the SPLMA deployment.

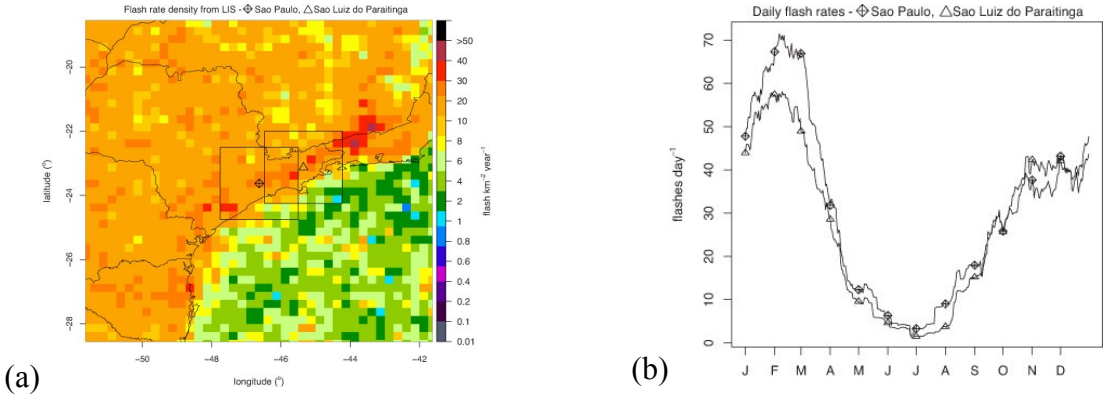

Figure 2 – (a) Lightning flash rate density (fl km^{-2} yr^{-1}) for Southeast Brazil. (b) Daily flash rate (flashes per day) around São Paulo and São Luiz do Paraitinga (i.e, flash rate over black squares (2 ¼º) around these cities on item (a)). Lightning data is from LIS climatology from 1 January 1998 to 31 December 2008 in ¼º of resolution.

The SPLMA deployment is intended to be completed by the end of October 2010, so that the onset of summer and the high lightning activity period can be monitored as shown in Figure 2. The length of the deployment will be from six months to one year. The SPLMA will consist of an 8-10 station network deployed in the vicinity of São Paulo. An 8-10 (or more) station LMA provides redundancy and increases overall robustness and signal detection, since not all receiving stations detect all the lightning signals. Spacing between stations is typically on the order of 15-30 km, with the network "diameter" being on the order of 80 km. Details on the NALMA and DCLMA, which show station spacing can be found at http://branch.nsstc.nasa.gov/PUBLIC/DCLMA/.

Figure 3 shows the preliminary layout for SPLMA, where the blue balloons are the suggested locations for 9 stations around the city of São Paulo. The red balloons are additional stations under consideration around the city of São José dos Campos, closer to CHUVA IOP site (São Luiz do Paraitinga – yellow "push pin"). The São José dos Campos LMA network is centered at INPE, where an instrumentation tower with high speed cameras and other instruments can add valuable information for GLM and CHUVA purposes. Since a LMA provides good 3D coverage out to 150 km, this coverage will overlap nicely with the areal coverage by the São Luiz do Paraitinga dual polarization radar (especially toward the west) that will be working at the area during this CHUVA IOP. LMA provides 2D detections

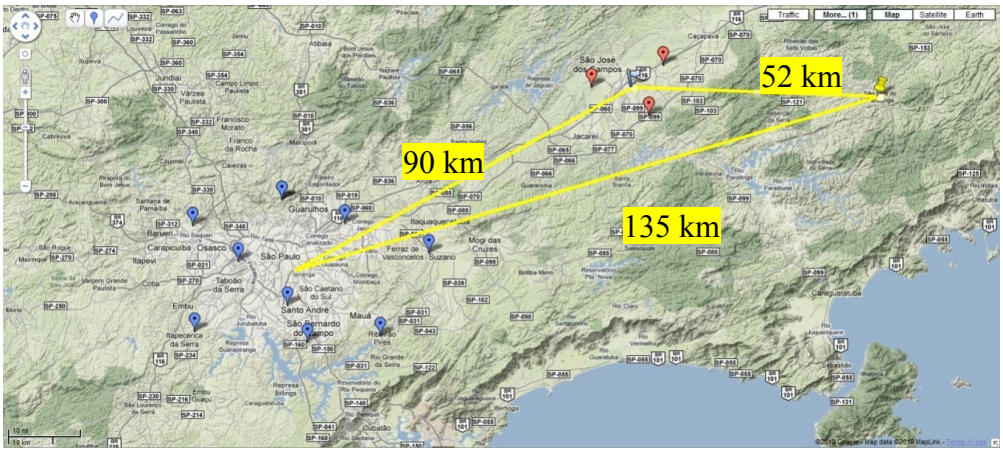

Figure 3 - Blue balloons show preliminary configuration for the SPLMA network for CHUVA. The red balloons show a second network configuration, centered at INPE (Sao Jose dos Campos). Yellow "push pin" is the São Luiz do Paraitinga CHUVA IOP site. Yellow lines show distance between the networks and CHUVA IOP.

out to 250+ km (and often detects lightning even farther away). LMA data will be processed and make available online through a SPLMA web site. The "modus operandi" for SPLMA will be very similar to that used by the DCLMA, in which all the stations are connected to the internet for real time collections, processing and display of decimated data, and post real time processing of the full data sets.

3 – CONCLUSIONS

The contribution of SPLMA will be to provide the CHUVA campaign with total lightning, lightning channel mapping and detailed information on the locations of cloud charge regions for the thunderstorms investigated during the São Luiz do Paraitinga IOP. Much of the lightning information will not be available without the LMA. The real-time availability of LMA observations will also contribute to and support improved weather situational awareness and mission execution. For GOES-R program it is a target-of-opportunity to acquire unique proxy data for GLM and ABI. The measurements obtained from SPLMA deployment will provide for the first time total lightning measurements in conjunction with SEVIRI observations. The data acquired through the combination of CHUVA IOP and the SPLMA will form the basis of generating unique and valuable proxy data sets for both GLM and ABI sensors in support of several on-going research investigations.

5 – REFERENCES

CECIL, D. J., S.J. GOODMAN, D.J. BOCCIPPIO, E.J. ZIPSER, S.W. NESBITT: Three Years of TRMM Precipitation Features. Part I: Radar, Radiometric, and Lightning Characteristics, Mon. Wea. Rev., 133, 543–566 (2005).

CHRISTIAN, H. J., and S. J. GOODMAN: Optical observations of lightning from a high altitude airplane, J. Atmos. Ocean. Tech., 4, 701-711 (1987).

CHRISTIAN, H. J., R. J. BLAKESLEE, S. J. GOODMAN, D. M. MACH: Algorithm Theoretical Basis Document (ATBD) for the Lightning Imaging Sensor (LIS), NASA (2000).

CHRISTIAN, H. J., AND CO-AUTHORS: Global frequency and distribution of lightning as observed from space by the Optical Transient Detector, J. Geophys. Res., 108, 4005, doi:10.1029/2002JD002347 (2003).

CUMMINS, K. L. AND M.J. MURPHY: An overview of lightning locating systems: History, techniques, and data uses, with an in-depth look at the U.S. NLDN. IEEE Trans. Electromagnetic Compatibility, 51(3), 499–518 (2009).

GATLIN, P. and S. J. GOODMAN: A total lightning trending algorithm to identify severe thunderstorms. J. Atmos. Oceanic Tech., 27, 3-22 (2010).

GOODMAN, S. J. , H. J. CHRISTIAN, W. D. RUST: Optical pulse characteristics of intracloud and cloud-to-ground lightning observed from above clouds, J. Appl. Meteor., 27, 1369-1381 (1988).

GOODMAN, S. J., D. E. BUECHLER: Lightning-Rainfall Relationships, Preprints of the Conf. on Operational Precipitation Estimation and Prediction, Anaheim, CA, Amer. Met. Soc., Boston, Feb. 7-9 (1990).

GOODMAN, S. J., AND CO-AUTHORS: The North Alabama Lightning Mapping Array: Recent severe storm observations and future prospects. Atmos. Res., 76, 423-437 (2005).

LIU, C., E. J. ZIPSER, D. J. CECIL, S. W. NESBITT, S. SHERWOOD: A Cloud and Precipitation Feature Database from Nine Years of TRMM Observations, J. Appl. Meteor. Climatol., 47, 2712–2728 (2008).

MAIER, L., C. LENNON, T. BRITT, AND S. SCHAEFER: LDAR system performance and analysis, in Proceedings of the International Conference on Cloud Physics, Am. Meteorol. Soc., Boston, Mass., Dallas, Tex., Jan 1995.

PETERSEN, W. A., S. A. RUTLEDGE: On the Relationship Between Cloud-to-ground Lightning and Convective Rainfall, J. Geophys. Res., 103, 14025-14040 (1998).

RISON, W., R. J. THOMAS, P. R. KREHBIEL, T. HAMLIN, AND J. HARLIN: A GPS-based three-dimensional lightning mapping system: Initial observations in central New Mexico, Geophys. Res. Lett., 26, 3573– 3576 (1999).

SCHULTZ, C. J., W. A. PETERSEN, L. D. CARREY: Preliminary Development and Evaluation of Lightning Jump Algorithms for the Real-Time Detection of Severe Weather. J. Appl. Meteorol. Climatol., 48, 2542-2563 (2009).

WILLIAMS, E. R., AND CO-AUTHORS: The behavior of total lightning activity in severe Florida thunderstorms. Atmos. Res., 51, 245–265 (1999).

ANEXO 15

The CHUVA Lightning Mapping Campaign

S. J.Goodman[1], R. J. Blakeslee[2], J. C. Bailey[3], L. D. Carey[3], H. Hoeller[4], R. Albrecht[5], L. Machado[5],C.A. Morales[6], O. Pinto Jr[7], M. Saba[7],K. Naccarato[7],S. Heckman[8], N. Hembury[9], Robert Holzworth[10]

[1]NOAA NESDIS GOES-R Program, NASA GSFC, Greenbelt, MD 20771, USA, e-mail: steve.goodman@noaa.gov
[2]NASA Marshall Space Flight Center, Huntsville, AL 35812, USA, e-mail: rich.blakeslee@nasa.gov
[3]University of Alabama in Huntsville, Huntsville, AL 35899, USA, e-mail: jeffrey.c.bailey@nasa.gov
[3]University of Alabama in Huntsville, Huntsville, AL 35899, USA, e-mail: larry.carey@nsstc.uah.edu
[4]DLR-Institut fur Physik der Atmosphaere, Oberpfaffenhofen, D-82234 Wessling, Germany
[5]Instituto Nacional de Pesquisas Espaciais, Cachoeira Paulista, SP Brazil , e-mail: rachel.albrecht@cptec.inpe.br
[6]Universidade de São Paulo, São Paulo, SP Brazil, e-mail morales@model.iag.usp.br
[7]Instituto Nacional de Pesquisas Espaciais, S. J. dos Campos, SP Brazil , e-mail: osmar@dge.inpe.br
[8]Earth Networks, Germantown, MD, e-mail: stan.heckman@gmail.com
[9]Vaisala, Inc., Tucson, AZ, e-mail nikki.hembury@vaisala.com
[10]University of Washington, Seattle, WA 98195, USA, e-mail: bobholz@ess.washington.edu

The primary science objective for the CHUVA lightning mapping campaign is to combine measurements of total lightning activity, lightning channel mapping, and detailed information on the locations of cloud charge regions of thunderstorms with the planned observations of the CHUVA (***C***loud processes of t***H***e main precipitation systems in Brazil: A contrib***U***tion to cloud resol***V***ing modeling and to the GPM (Glob***A***l Precipitation Measurement) field campaign. The lightning campaign takes place during the CHUVA intensive observation period October-December 2011 in the vicinity of São Luiz do Paraitinga with Brazilian, US, and European government, university and private sector participants. Thunderstorms occur regularly at this location and season, associated with the South Atlantic Convergence Zone (SACZ), local convection, and orographic enhancement of precipitation. Total lightning measurements that can be provided by ground-based regional 2-D and 3-D total lightning mapping networks coincident with overpasses of the Tropical Rainfall Measuring Mission Lightning Imaging Sensor (LIS) will be used to generate proxy data sets for the next generation US and European geostationary lightning mappers, currently in development at NOAA and EUMETSAT. Proxy data, which play an important role in the pre-launch mission development and in user readiness preparation, are used to develop and validate algorithms so that they will be ready for operational use quickly following the planned launch of the GOES-R Geostationary Lightning Mapper (GLM) in 2015 and the Meteosat Third Generation Lightning Imager (LI) in 2017. Both the US and European satellites will also have more advanced 16-channel imagers to provide higher resolution cloud imagery and more detailed, rapid update information on cloud properties. Additional proxy data and products for these next generation imagers can be produced from the SEVIRI (Spinning Enhanced Visible and Infrared Imager) on the Meteosat Second Generation satellite in geostationary earth orbit and the low-earth orbiting Moderate Resolution Imaging Spectro-radiometer on the NASA Terra and Aqua satellites, all of which view the southeast portion of Brazil. To date there is no *well-characterized* total lightning data coincident with the imagers. Therefore, to take the greatest advantage of this opportunity to collect detailed and comprehensive total lightning data sets, test and validate multi-sensor nowcasting applications for the monitoring, tracking, warning, and prediction of severe and high impact weather, and to

advance our knowledge of thunderstorm physics, extensive measurements from a São Paulo VHF Lightning Mapping Array (SP-LMA) network will be augmented with several additional lightning networks and ancillary measurements, including the WeatherBug Total Lighting Network (WTLN), DLR LINET network, Vaisala TLS200, World Wide Lightning Location Network (WWLLN), Vaisala GLD360, WSI Precision Lightning Data Network, and the National Lightning Detection Network of Brazil (RINDAT) in conjunction with electric field mills, field change sensors, high speed cameras and other lightning sensors, dual-polarimetric radars, and aircraft in-situ microphysics which will allow for excellent cross-network inter-comparisons, assessments, and physical understanding.

*Corresponding author: NSSTC/UAH, NOAA/NESDIS, 320 Sparkman Dr, Huntsville, AL 35805, PH: 202-380-8164, E-mail: steve.goodman@noaa.gov